TAMPEREEN TEKNILLINEN YLIOPISTO
TAMPERE UNIVERSITY OF TECHNOLOGY

SHAHBAZ AHMED

INTEGRATION OF AN RFID READER ANTENNA WITH A WORK GLOVE

Master of Science Thesis

Examiner: Academy Research Fellow Toni Björninen and Professor Leena Ukkonen
Examiner and topic approved by the Faculty Council of the Faculty of Computing and Electrical Engineering on 20 January, 2018

ABSTRACT

SHAHBAZ AHMED: Working antenna for gloves
Tampere University of technology
Master of Science Thesis, 66 pages
January, 2018
Master's Degree Programme in Electronics Engineering
Major: Electronics Engineering
Examiner: Academy Research Fellow Toni Björninen and Professor Leena Ukkonen
Keywords: UHF RFID, Wearable Antenna, Split Ring Antenna, Slotted Patch Antenna and Body Area Network

RFIDs are widely deployed in the daily life and its application has been growing with the development of the technologies. RFID application includes everything from the card payment systems to military purposes. In the recent decades, there is significant work done on the tags and various tags have been developed depending on the application requirements, but not much work has been done on the wearable RFID readers. A significant step toward making the RFID reader wearable is to develop wearable RFID reader antenna with considerable read range

In this thesis, two types of antennas—slotted patch antenna and split ring resonator antenna—are fabricated and their performance on the human hand is analyzed. The material selected as a substrate is EPDM foam material with permittivity 1.26 and tangent loss 0.007. The thickness of the substrate differs in fabrication of both the antennas. In case of slotted patch antenna, the substrate thickness is 4mm, whereas, in case of split ring resonator antenna, the thickness of the substrate is 3mm. The material of the radiating element needed to be flexible and with good conductivity. For this reason, nickel platted conductive textile with sheet resistance 0.16Ω/square is used for fabrication.

The summary of the results shows the designed antenna are capable of operating on the desired frequency range. However, the SRR antenna is more flexible, lightweight and bendable with the same read range. For the free space measurement, both the antennas showed good agreement between the measured and simulated results. However, due to inaccuracies in the fabrication of the antennas, the resonance frequency is shifted to other frequencies. In addition to that, bending in two planes i.e xz and yz planes, are performed and results are measured. It is observed that the bending effects the return loss and bandwidth of the antenna, when the antenna is bending is along the effective length of the antenna. The reason for the resonance frequency shifting is that it changes the slot dimension of the antenna, which ultimately effects the current path on the antenna surface. Both antennas showed nearly equal read ranges when the Voyantic Reference tag is measured with both the antennas.

PREFACE

The master thesis, “Integration of an RFID reader Antenna with a Work Glove” was done in partial fulfillment of the requirement for the Masters of Science degree in Electronics Engineering major, in the Department of Electronics and Communication Engineering at Tampere University of Technology. All the research and investigation has been made in the Wireless Identification and Sensing Systems Research Group (WISE) under the supervision of Prof. Leena Ukkonen and Academy Research Fellow Toni Björninen. I would like to thank my thesis examiners and supervisors, Prof. Leena Ukkonen and Academy Research Fellow Toni Björninen, for all of their support, continuous guidance and for proving me an appropriate environment to complete my thesis. I would like to thank to all my colleagues in the WISE Group for their help and support.

First and foremost, I am thankful to mighty for giving me strength to learn and understand the diverse technologies and helping me to complete this research work on time. I am very thankful to my friends specially Muhammad Waqas Ahmed Khan, Muhammad Rizwan, Shahzad Ahmed, Zeeshan Ahmed and Raghda Hamed for their help during my measurements. I would like to thank my family for their continuous support to make this thesis possi-ble.

Tampere, January 2018

Shahbaz Ahmed

CONTENTS

LIST OF FIGURES

LIST OF SYMBOLS AND ABBREVIATIONS

RFID	Radio Identification Technology
UHF	Ultra High Frequency
BAN	Body Area Network
EPDM	Ethylene Propylene Diene Monomer
PLF	Polarization Loss Factor
RL	Return Loss
BW	Bandwidth
QF	Quality Factor
LF	Low frequency
HF	High Frequency
PIE	Pulse Integral Encoding
ISM Band	Industrial, Scientific and Medical Band
PDA	Personal Digital Assistant
SRR	Split Ring Resonator
HFSS	Institute of Electrical and Electronics Engineers
dB	Decibel
VNA	Vector Network Analyzer
PIFA	Planar Inverted F Antenna
R	Real Impedance
X	Imaginary Impedance
E	Electric Field
H	Magnetic Field
ε	Permittivity
δ	Loss tangent factor
P	Polarization density
χe	Electric susceptibility
D	Electric displacement field
μ	Permeability
C	Speed of light
ξ	Instantaneous field
ϕ	Linear Polarization
$\hat{p}$	Unit vector
D	Maximum dimension of antenna
τ	Impedance mismatch
Z	Complex Impedance
D	Directivity
G	Gain
P	Power of transmitted or received

1. INTRODUCTION

Radio Frequency Identification Technology (RFID), as depicted, utilizes the electromagnetic waves from the reader and a small transponder to respond to queries by transmitting a specific serial number or identifier code. RFID overcame shortcomings—like alignments, read range, limited data storage capacity and environmental effects—of already deployed identification systems including Barcode, Optical Character Recognition, Voice Recognition, Biometry, and Smart Card by identifying and tracking objects using radio waves. RFID technology has an advantage over other technologies with distant and parallel interrogation at once, enhanced security, and no line of sight required [1]. A RFID system consists of small transponders called tag, a reader, and a back-end server. The retrieved identification code from the tag does not provide much information nor can it keep track of the items unless it is combined with a back-end storing the descriptive information about the tags. When the RFID readers, receive the tag response, it compares the code with the descriptive information from the database and displays it on the user interface [2]. Nowadays, with the advancement in the wearable and flexible electro-textile, RFID technology—both readers and the tags—has been implemented for different Body Area Networks (BANs) using different wearable materials. These BAN RFID devices can be used for physiological changes within and outside the body, diagnostic of the brain disease, biomedical healthcare applications, the item inventory, access control, in the logistics, and supply chain management purposes [1]. The frequency band used for the Ultra-High Frequency (UHF) RFID system is 860-960 MHz [3]. Wearable flexible materials are used for manufacturing of the BAN devices to cause minimum hindrance to the body movement. Most of the wearable antenna developed are mostly non- flexible [4], thick substrate [5], large sized [6] and linearly polarized. In Bio-medical applications involving the RFID technology, the signal is transmitted from on-body unit to the off-body unit using a wireless link, established between the two transceivers. The problem arises due to the high lossy electrical properties of the human tissue, which weakens the radio link between the tag and the reader. Nowadays, RFID systems can be designed for different body parts, which can serve various purposes.

Aim of the project:

In this thesis, the main objective is to develop RFID Split Ring Resonator (SRR) and Slotted Patch reader antenna, mountable on working hand gloves, using nickel and copper plated electro-textile that is flexible and wearable material on EPDM material of 3mm and 4mm thickness respectively. The antenna will be integrated with the RFID reader. The main objective is to attain the maximum read range for the reader antenna in close vicinity of the body. As the requirement of this application is to design a compact small antenna comparable of hand size with the desired read range, hence two types of antennas were selected; SRR and the slotted patch antenna. This documentation, in addition to the individual performance of the antennas provides, the comparison of these two antennas

in term of gain, directivity, maximum read range, radiation pattern, and size. The figure 1-2 shows, the operation mechanism of the project.

Development Approach:

The development approach used to design the antenna is iterative method, shown in the figure, to get the most optimized outcomes of the project.

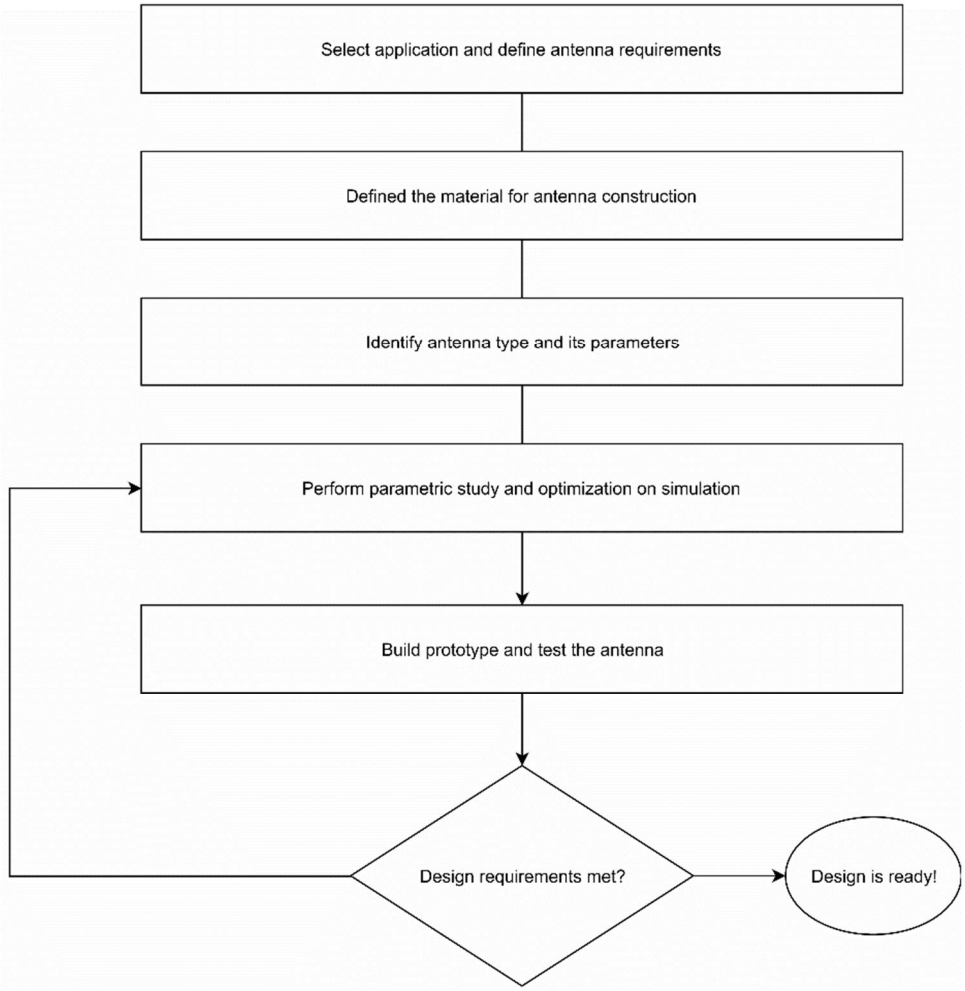

Figure 1-1 *Development approach used for designing of the antenna*

Challenges:

The main challenges in designing and implementation of the wearable antennas are:

- The body acts as a lossy material and reduced the gain of the antenna.
- The size of the antennas should be small which can be achieved by using miniaturization techniques; however, miniaturization can greatly reduce the efficiency of the antennas.
- Due to the reduced gain and efficiency, the read range of the reader antenna might also reduce.

Chapter 2 includes the basics of the antennas and the electromagnetic theory. Chapter 3 discussed gives a general idea about the RFID systems and importance of the reader antenna and motivation of the project. Chapter 4 emphasis on the wearable technology. In chapter 5, the simulation and designing aspects of both SRR and the slotted patch antenna is discussed. Chapter 6 and 7 both describes the free space and on-body measurements of both antennas. Chapter 8 includes the comparison between both antennas, for example, size, bending and efficiency of the reader antennas. The chapter 9 concludes the thesis and give a summary of the research work done along with future improvements that can be made.

2. ELECTROMAGNETIC THEORY AND ANTENNAS

The electromagnetic theory is of core importance for in-depth understanding about the antennas, their electromagnetic fields, and wave propagation. The term electromagnetism refers to the rate of change of current, exhibiting particular frequency [7]. The Maxwell equation sums up the relation between the electro-magnetic fields with the current and electric charges. In 1864, James Clerk Maxwell purposed his theoretical model called "Maxwell Equations" considering all the previous theoretical laws related to the electric and magnetic field to explain the magnetic phenomena. The Maxwell Equations proved themselves a step forward toward the industrial revolution.

2.1 Maxwell Equations

The Maxwell Equations describes how the electric charges give rise to electromagnetic forces per unit charge. Maxwell Equations comprise of four equations—integral, differential and phasor forms—defining the electromagnetic fields in the time and space coordinate systems.

Table 2-1 Maxwell Equations in Differential, Integral and Phasor form *[7]*

Differential form	Integral form	Phasor form	Designation
$\nabla \times \boldsymbol{E} = -\frac{\partial \boldsymbol{B}}{\partial t}$	$\int_{\partial S} \boldsymbol{E} \cdot d\boldsymbol{l} = -\frac{\partial}{\partial t}\int_{S} \boldsymbol{B} \cdot d\boldsymbol{s} \, \forall S$	$\nabla \times \boldsymbol{E} = -j\omega \boldsymbol{B}$	Faraday's law
$\nabla \times \boldsymbol{H} = \boldsymbol{J} + \frac{\partial \boldsymbol{D}}{\partial t}$	$\int_{\partial S} \boldsymbol{H} \cdot d\boldsymbol{l} = \int_{S} \boldsymbol{J} \cdot d\boldsymbol{s} + \frac{\partial}{\partial t}\int_{S} \boldsymbol{D} \cdot d\boldsymbol{s} \forall S$	$\nabla \times \boldsymbol{H} = \boldsymbol{J} + j\omega \boldsymbol{D}$	Ampère-Maxwell's law
$\nabla \cdot \boldsymbol{D} = \rho$	$\int_{\partial V} \boldsymbol{D} \cdot d\boldsymbol{s} = \int_{V} \rho \, dv = Q \, \forall V$	$\nabla \cdot \boldsymbol{D} = \rho$	Gauss' law for electricity
$\nabla \cdot \boldsymbol{B} = 0$	$\int_{\partial V} \boldsymbol{B} \cdot d\boldsymbol{s} = 0 \, \forall V$	$\nabla \cdot \boldsymbol{B} = 0$	Gauss' law for magnetism

Quantity	Symbol	Unit
Electric field intensity	$\boldsymbol{E}$	V/m
Magnetic field intensity	$\boldsymbol{H}$	A/m
Electric flux density	$\boldsymbol{D}$	Coul/m^2
Magnetic flux density	$\boldsymbol{B}$	Wb/m^2
Electric current density	$\boldsymbol{J}$	A/m^2
Electric charge density	ρ	Coul/m^3

Faraday's law states that the changing magnetic field gives rise to the electric field and Ampere's law states that the changing electric field—due to the flow of alternating current—gives rise to the magnetic field. For electricity, Gauss's law defines the electric flux variations around moving electric charges. The fourth equation is Gauss's law for magnetism, which states that the net magnetic flux through a closed volume is always zero and magnetic charge does not exist [8].

Linear materials having permittivity and permeability independent of the applied magnetics and electric fields, the constitutive relation exists

$$\boldsymbol{D} = \varepsilon \boldsymbol{E}, \tag{2.1}$$

$$\boldsymbol{B} = \mu \boldsymbol{H}, \tag{2.2}$$

$$\boldsymbol{J} = \sigma \boldsymbol{E}, \tag{2.3}$$

where ε, μ and σ are the permittivity, permeability, and conductivity of the material. Real time electromagnetic problems involve conterminous region of materials exhibiting different electrical properties which makes it necessary to satisfy the boundary condition for the field vectors. The boundary conditions for two conterminous materials can be found through the application of Maxwell equations. The Maxwell predicted the existence of the propagating electromagnetic waves through a medium or vacuum, based on his model.

2.1.1 Permittivity

The ***permittivity***, denoted by ε, exists between electric displacement and electric field intensity. Mathematically expressed as

$$\varepsilon = \varepsilon_r \varepsilon_o, \tag{2.4}$$

where $\varepsilon_r$and $\varepsilon_o$is the relative permittivity and dielectric constant. The electromagnetic material as also characterized, along with the relative permittivity, by the loss tangent factor that is dependent on the frequency and is referred as "measure of the power losses in a material and is the imaginary part of the complex permittivity" [9]. Mathematically

$$\tan \delta_e = \frac{\sigma_e}{\omega \varepsilon'} = \frac{\sigma_s}{\omega \varepsilon'} + \frac{\varepsilon''}{\varepsilon'}, \tag{2.5}$$

In the loss tangent, there are two terms; the first one due to collusion of electrons and the second term refers to dipole rotation as the dipoles inside the dielectrics cannot instantaneously respond to the external electric field. In general, the second term dominates due to the presence of the fewer free electrons in the dielectrics.

The ***electric susceptibility*** indicates the polarization of the dielectric material, when subjected to external electric field. The electric susceptibility is dimensionless. The susceptibility has a direct proportional relation with the polarization of the medium, greater the electric susceptibility; greater will be the material polarization. In general

$$\boldsymbol{P} = \varepsilon_0 \chi_e \boldsymbol{E}, \tag{2.6}$$

Where **P**, ε_o and **E** is the polarization density, electric permittivity of free space and applied electric field respectively. χ_e is the electric susceptibility of the material. The relationship between the electric permittivity and susceptibility is given by

$$\chi_e = \varepsilon_r - 1, \tag{2.7}$$

Where in case of vacuum χ_e equals to zero.

The electric displacement field **D** in the Maxwell's equation 2.1, is a vector field, which accounts for effects of the bounded and free charges within a medium. The bounded charges of dielectric materials in the presence of an external electric, tends to create dipoles within the material by slight displacement **D**, expressed as

$$\boldsymbol{D} = \varepsilon_o \boldsymbol{E} + \boldsymbol{P}, \tag{2.8}$$

Where **P** is the polarization density of the electric dipole induced in the material. It may also include the permanent dipoles of the material. The electric displacement field satisfies the equation

$$\nabla \bullet \mathbf{D} = \boldsymbol{\rho}, \tag{2.9}$$

In homogenous, isotropic and linear dielectrics the polarization density **P** depends on the electric field linearly, such that

$$\boldsymbol{P} = \varepsilon_0 \boldsymbol{\chi} \boldsymbol{E}, \tag{2.10}$$

Therefore,

$$\boldsymbol{D} = \varepsilon_o (1 + \chi) \boldsymbol{E} = \varepsilon \boldsymbol{E}, \tag{2.11}$$

Permeability, another term related to the material properties, is ability of a material to magnetize itself in the presence of external magnetic field. Permeability is an analogous quantity to permittivity and defined similarly from equation 2.2.

2.1.2 Polarization

Polarization of an antenna in any direction is the polarization of the transmitted wave in that direction [10]. In practical as the radiated energy differs in every direction with reference as center of the antenna, the polarization may also change. The orientation of the electric field vector at a specific time instant and given coordinates in the space is known as polarization of the wave. For transverse electromagnetic waves, the polarization is taken in the direction of maximum gain. The electromagnetic waves can exhibit three types of polarization; linear, circular and elliptical. [11]. An instantaneous field travelling in negative z direction is expressed as,

$$\xi(z;t) = \boldsymbol{a}_x \xi_x(z;t) + \boldsymbol{a}_y \xi_y(z;t), \tag{2.12}$$

Instantaneous components in x and y directions can be expressed as

$$\xi_x(z;t) = Re\left[E_x^{-} e^{j(wt+kz)}\right] = E_{xo}\cos(\omega t + kz + \phi_x), \quad (2.13)$$

$$\xi_y(z;t) = Re\left[E_y^{-} e^{j(wt+kz)}\right] = E_{yo}\cos\left(\omega t + kz + \phi_y\right), \quad (2.14)$$

$$\xi(z;t) = E_{xo}\cos(\omega t + kz + \phi_x) + E_{yo}\cos\left(\omega t + kz + \phi_y\right), \quad (2.15)$$

Where $\xi_x \; and \; \xi_y$ are the x and y components of instantaneous field travelling in negative z direction respectively.

Linear Polarization:

A wave is said to be linearly polarized, if the electric field vector always points along a straight line at every moment. In linear polarization, the electric field vector moves back-ward and forward along a fixed line, as depicted in figure 2-3. The Linear polarization can be achieved if the following conditions for electric field possess only one component or two orthogonal components, in phase with each other or out of phase in multiples of 180° or two orthogonal components, in phase with each other or out of phase in even multiples of 180°. Such that in equation 2.16. In case of linear polarization, axial ratio is infinity.

$$\Delta\phi = \phi_y - \phi_x = n\pi \qquad n = 0,1,2,3 \ldots, \quad (2.16)$$

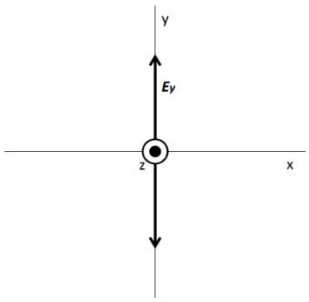

Figure 2-1 *linearly polarized wave*

Circular Polarization:

The circular polarization are limited cases of the elliptical polarization. When the electric field vector of a time varying wave traces as a circle that is function of time, the wave is circularly polarized. To achieve the circular polarization the electric field vector should have two orthogonal components that should be linear and should have same magnitudes. In addition to this, these components should be out of phase with each other by 90° or by its odd multiples. Such that in equation 2.16

$$|\xi_x| = |\xi_y|,$$

$$\Delta\phi = \phi_y - \phi_x = +\left(\frac{1}{2} + n\right)\pi \qquad n = 0,1,2,3 \ldots, \quad (2.17)$$

$$\Delta\phi = \phi_y - \phi_x = +\left(\frac{1}{2} + n\right)\pi \qquad n = 0,1,2,3\ldots, \qquad (2.18)$$

Where equation 2.17 refers to the clockwise and the equation 2.18 refers to the counter clockwise rotation.

Circular polarization is illustrated in figure 2.2-2(b), the electric field vector remains constant but rotates in circular form with a constant angular frequency ω. The angular frequency also defines the left-hand and right-hand polarization depending upon the direction of rotation, clock-wise or anti-clockwise respectively.

Elliptical Polarization:

In case of Elliptical polarization, the tip of electric field vector follows an elliptical trace in space. At any instant of time, the electrical field vector points the corresponding elliptical locus. The elliptical polarization illustrated in the figure 2-4(a). The polarization is right handed or left handed if the electric field vector rotates clockwise or counter-clock wise respectively. Axial ratio (AR) is the ratio of the major to minor component of electric fields and ranges from one to infinity. The axial ratio equal to one, factor characterizes the Elliptical polarization.

To achieve the elliptical polarization, the electric field vector must have two orthogonal linear components with same of different magnitudes. If the electric components are of same magnitude then they should not in phase with each other or the time phase difference should be either zero or multiples of 180°. In case the electric field components are of different magnitude, then the time phase difference between the orthogonal components should not be odd multiples of 90°, which is the case of circular polarization.

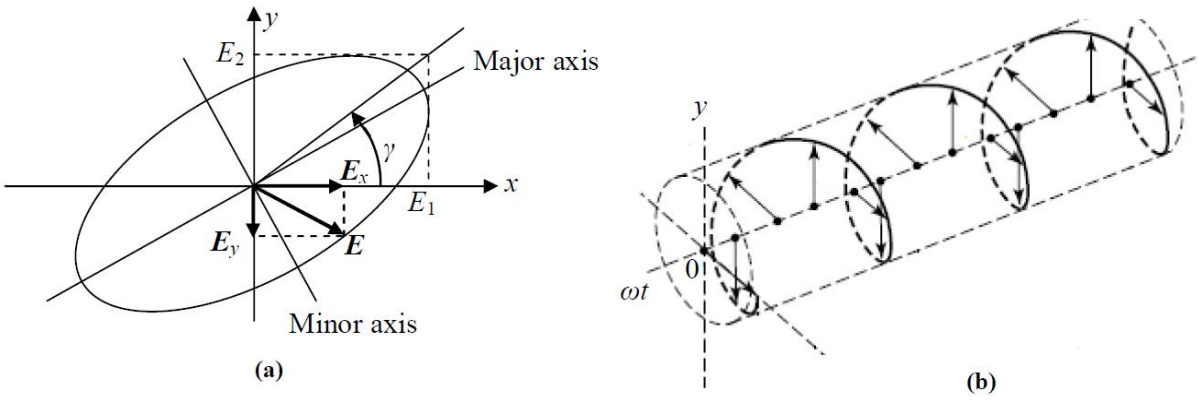

Figure 2-2 (a) Elliptical polarization (b) Circular polarization ***[10]***

Polarization of an antenna is the polarization of the transmitted electromagnetic wave in a specific direction that is typically in the direction as that of maximum gain [10]. The

polarization of an antenna remains constant over the main beam, but it can significantly differ for the minor lobes [12].

Polarization Mismatch:

In Practical, the polarization of the incident wave may differ from the polarization of the receiving antenna. In this case, the power extracted by the antenna from the incident wave might not be maximum, because of the different polarization known as *polarization mismatch*.

$$\boldsymbol{E}_i = \hat{\rho}_{\boldsymbol{\omega}} E_i, \tag{2.19}$$

$$\boldsymbol{E}_a = \hat{\rho}_{\boldsymbol{a}} E_a, \tag{2.20}$$

Where the E_i and E_a refers to the electric field of incoming wave and the electric field of the receiver antenna respectively. $\hat{\rho}_{\boldsymbol{\omega}}$ and $\hat{\rho}_{\boldsymbol{a}}$ are the unit vector of incident wave and unit vector of receiver antenna respectively also known as polarization vectors [10]. Polarisation loss factor PLF, which is the measure of polarization mismatch can be defined as

$$PLF = |\hat{\rho}_{\boldsymbol{\omega}} \bullet \hat{\rho}_{\boldsymbol{a}}|^2 = |\cos \Psi_p|^2 \ , \tag{2.21}$$

Where Ψ_p is the angle between the two vectors form the angle. When the *PLF* is 0.5 then half of the power is delivered, whereas, when the *PLF* is 0, the no power is transferred. In case of maximum power transfer by the antenna, the *PLF* is unity.

2.2 Antenna Theory

Antenna is a reciprocal device capable of transforming the electrical signals into electromagnetic waves and vice versa. Antennas are one of the most significant components of modern wireless communication systems [13]. In addition to energy transformation, antennas should transmit the energy in a specified direction and suppress in other directions. When antenna is acting as transmitter, time varying current flow through the antenna and generates electromagnetic waves, whereas, in reception, time varying electromagnetic waves induces alternating current in the antenna. Antenna is a passive device—exhibiting no gain as it does not amplify signal—that can receive and transmit wave energies to establish a wireless link between multiple devices.

2.2.1 Radiation Mechanism

According to Maxwell, when the charges accelerates or decelerates in unit area, radiation are generated. Therefore, for generation of space free electromagnetic waves, we need to flow a time varying electromagnetic field, through a transmission line. When these two conditions are fulfilled, the electromagnetic waves are generated and spread in all direc-

tions [9]. The radiation region can be categorized into two; near and far field [10]. However, the near field is further, categorized in reactive and radiated near field. The reactive near field region is the vicinity, where the reactive field dominates, and is at a distance R from the antenna surface, where R<$0.62\sqrt{\frac{D^3}{\lambda}}$ [9]. The region where the field distribution depends on the distance R from the antenna. This is also called Frensel region and spreads over distance R, such that $0.62\sqrt{\frac{D^3}{\lambda}} < R < \frac{2D^2}{\lambda}$ [9]. In far field region, the radiation waves propagate can be approximated as plane waves and does not change shape. This region spread over a range $\frac{2D^2}{\lambda} < R < \infty$. The figure 2-5 shows the field regions surrounding the antennas.

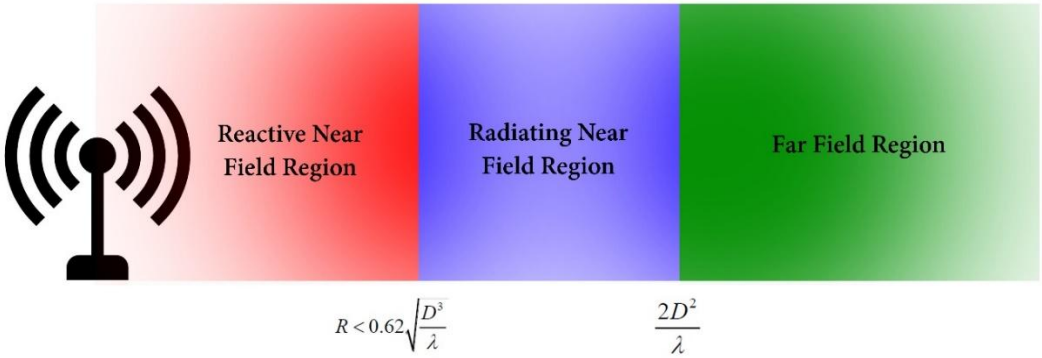

Figure 2-3 *Radiation field regions surrounding antennas*

2.2.2 Input Impedance

The input impedance is ratio between the antenna terminal voltage and current which may exist in a complex form exhibiting an imaginary and a real part. The real part corresponds the energy either radiated away from antenna or dissipated with in the antenna in the form of heat. The complex part represents the power stored in the near radiation field [14] and equivalent impedance model of an antenna is shown in the figure 2-6.

$$Z_A = R_A + j\, X_{A,} \tag{2.22}$$

The maximum power transfer occurs when the load impedance $Z_L = R_L + jX_L$ and the antenna input impedance is conjugate match of each other [15], such that $Z_A = Z_L^*$. Once the conjugate matching is achieved, the half of the power available in the antenna is delivered to the antenna which is radiated by the internal radiation resistance and the other half of the power is dissipated in the internal resistance as heat. However, as the input impedance of the antenna is frequency dependent, therefore, impedance matching can be

achieved over a limited bandwidth. The antenna input impedance depends upon excitation, geometry, substrate, and other elements surrounding the antenna.

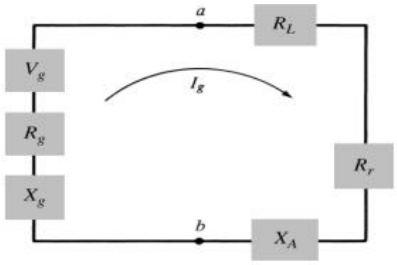

Figure 2-4 *Equivalent circuit of an antenna* ***[16]***

2.2.3 Return Loss and Impedance Mismatch

Return loss of antenna is the power reflected back from the terminal, when the antenna is mismatched. In general, the return loss of the antenna is -10dB, which suggests that ninety percent of the power will be delivered to the antenna for radiation. Mathematically

$$RL_{(dB)} = -10log_{10}|\Gamma|^2, \tag{2.23}$$

Better the return loss of the antenna, more the power will be transmitted. Conjugate matching should be achieved to ensure minimize the return loss of the antenna.

Different type of impedance matching techniques can be used for matching. The mismatch can be calculated with the help of power transmission coefficient, which is account of mismatch between the antenna and the load. The factor is given by [17]

$$\tau = \frac{4R_L R_A}{|Z_L+Z_A|^2}, \tag{2.24}$$

Where $Z_A=R_A+jX_A$ and $Z_L=R_L+jX_L$ is the impedance of the tag antenna and the load respectively. As the $\tau = 1-|\Gamma|^2$, therefore [18]

$$\Gamma = \frac{Z_A-Z_L^*}{Z_A+Z_L}, \tag{2.25}$$

As for maximum power transfer, the impedance matching is an important task, which implies that the antenna impedance should have inductive impedances as load will have capacitive impedance. This is also referred as conjugate impedance matching, which can be done by multiple techniques. Several methods are used for impedance matching including lumped component circuit, transmission line transformers and either by modifying the antenna structure.

2.2.4 Radiation Pattern

Radiation pattern, a far field property, is the graphical representation of radiation properties of an antenna—usually scaled in dB—in space coordinates. Figure 2-7 shows the radiation pattern in spherical coordinate systems. However, in most of the cases, a two-dimensional, transversal view of a 3D radiation pattern can provide the required information. In general, at each point near the antenna position, three coordinates of the electric field exist, E_θ, E_φ and $E_r$defining the magnitude of the electric field. However, the radial component reduces to zero in the far field regions. Different properties of antenna can be represented in the form of radiation pattern such as, field pattern and power pattern in linear scale or decibel scale represents magnitude of electric or magnetic field and its square as a function of the spherical coordinates. However usually the radiation patterns are usually scaled in decibels.

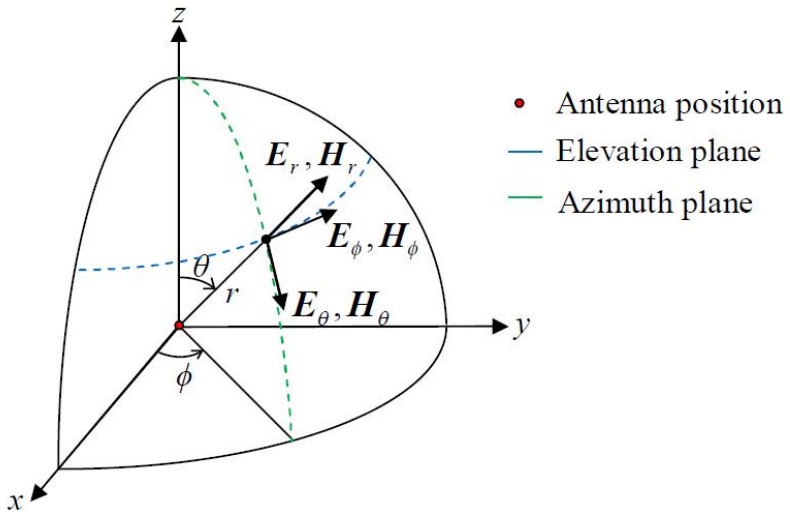

Figure 2-5 *Field components in spherical coordinate system* [10]**.**

Radiation pattern comprises of two of more parts referred to as lobes which can further divided into minor, main, side, and back lobes as shown in figure 2-8. The main lobe is always in the direction of maximum radiation and the minor lobes are the lobes on both sides of the main lobe. Back lobes are usually in the opposite direction of the main lobe. The side lobes are in any direction and always in between the minor lobe and the back lobes. The Beam Width, another terminology used is the angular width, measure in degrees or radians, where the radiated power becomes -3dB of the maximum power and the bandwidth of the beam width is known as -3dB bandwidth or Half Power Band Width HPBW.

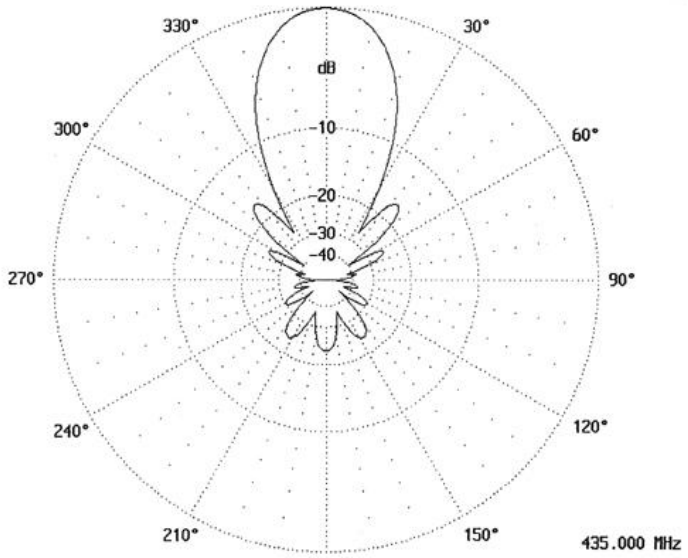

Figure 2-6 *Radiation pattern of an antenna in Polar form*

The radiation pattern can be categorized into three; isotropic, directional, and omnidirectional. An isotropic is an ideal pattern, radiation equally in all directions, however, the directional antennas radiates effectively in specific direction only. In general, directional antennas has more directivity than that of a dipole antenna [9]. The figure 2-8 shows the radiation pattern of a Yagi antenna at 435MHz frequency.

2.2.5 Directivity and Gain

Directivity of an antenna is how efficiently the antenna is transmitting power in a given direction. In case of the ideal antenna, the directivity becomes equal to the gain of the antenna. Directivity can also be expressed as the ratio of maximum power to the average power radiated [9].

$$D = \frac{P_{max}}{P_{avg}}, \tag{2.26}$$

Directivity and radiation of an antenna are related to each other. Low directivity means the antenna radiates in all direction more or less with equal magnitude, whereas, high directivity depicts that the antenna radiates more in one direction over larger distance.

As the antenna is a passive device, which means it cannot amplify the signal it radiates. However, term gain is usually associated to the antenna gain, which can be defined as the capability of antenna to radiate the power available at its terminal and is expressed in decibels. Gain and directivity are directly proportional to each other, provided the efficiency is constant over the bandwidth *k*.

$$G=kD, \tag{2.27}$$

2.2.6 Friis Transmission Formula

Fris transmission formula is used to relate the transmitted and radiated power between two distance antennas and can be expressed in various forms. In general

$$\frac{P_r}{P_t} = e_{rr} D_r e_{rt} D_t (1 - |\Gamma_r|^2)(1 - |\Gamma_t|^2) \left(\frac{\lambda}{4\pi R}\right)^2 PLF, \tag{2.28}$$

Where subscripts t and r represent the transmitter and receiver antennas respectively. As shown in the figure 2-9, distance R is the separation distance between two antennas. The Friis formula is applicable in the far field regions.

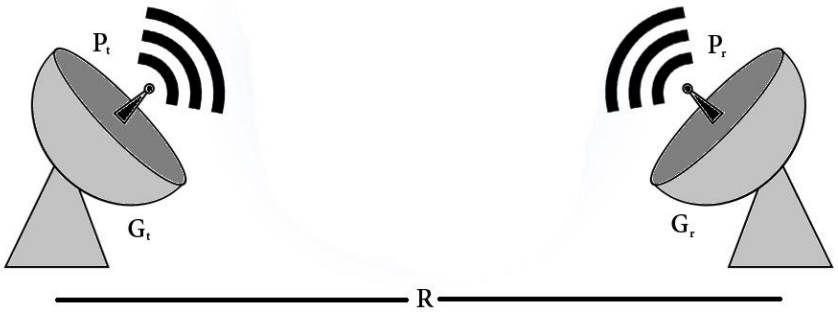

Figure 2-7 *Setup for the Friis formula*

Another form of the Friis formula can be derived, however, assumptions are to be made that there is no reflection between the antennas having same polarization, such that Γ_t^* and Γ_r^* are both zero.

$$\frac{P_r}{P_t} = G_r G_t \left(\frac{c}{4\pi R}\right)^2, \tag{2.29}$$

3. RFID BASICS

In 1948, a point-to-point communication was purposed between two nodes using the power of carrier and modulated reflector, which was not implementable at that time due to its dependency on the technologies like communication and application specific integrated circuits [19]. However, since after 1970s, the research and development in the field of RFID started [20]. After the invention in late 70s, RFID is now used for number of applications in everyday life in all the practical fields from logistics to security systems. RFID technology comprises of a RFID tag and a Reading device capable of reading RFID tag. Furthermore, RFID tag has a miniaturized antenna, an ASIC chip and a power source depending upon the RFID type.

Categorically RFIDs may be passive, semi-active or active depending whether they are powered by some internal source or not. Active RFIDs has continuous availability of power however, semi-active and passive RFIDs have availability of power within the range of the reader. On the other hand, RFIDs can be classified on their operational frequency basis as LF, HF or UHF. Now a days, passive UHF are widely known for the practical application because of the compact design, long range readability, fast data transferring rate, cost effectiveness, better performance and less interference when application specifically designed. For example, UHF RFID can be designed for in close metal proximity and its performance can be enhanced by using metal conductivity performances. Typically, UHF RFIDs operate in 860-960MHz frequency range in US [21] and 865-868 MHz in Europe. The most challenging factor in RFID technology is to design an antenna that should resonate on the desired frequency with various kinds of materials including metallic and flexible materials and meet the application specific characteristics like impedance, radiation pattern, antenna size, read range, polarization and gain. In passive RFIDs, the antenna should have impedance matching with the ASIC circuitry and should generate enough power to turn on the electronic circuitry and for backscattering. However, the reader antenna is designed with input impedance 50Ω.

Currently, International Standard Organization ISO and Electronics Product Code Global Incorporated EPCgloble are working on the standardization of RFID. Both of these organizations are working on defining the series of standards for RFID systems including the communication protocols, data content and air interference etc, which helps different manufacturers of RFID systems to work together [22].

3.1 RFID System

Typical RFID system is shown in the figure 3-1, comprising of a transponder or tag, a RFID antenna along with a reader and a backend server. The data or code extracted from the tag, does not give the necessary information, unless the gathered information is combined with the backend console system. The backend console is a high-end server machine storing the data corresponding to the each tag code. The backend is also responsible

for establishing the radio link with the tag. The reader is meant for transmitting power and interrogation of the signal to the tag. The tag usually comprises of a meandered antenna attached to application specific integrated circuit, which turns on by the energy from the transmitted signal. The tag sends back the information stored in it memory back to the reader through the meandered antenna.

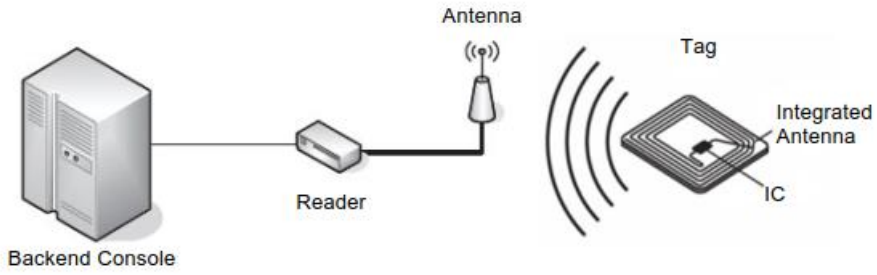

Figure 3-1 *Typical RFID system with Backend console* ***[15]***

RFID system communicate with the tag through a duplex channel—which includes encoding, decoding, modulation and demodulation—downlink and uplink transmission channel. The uplink channel is used to communicate from the tag to the reader, whereas, the downlink channel is used to communicate from the reader to the tag, carrying the required information from the reader and, most importantly, the continuous amount of energy required to turn on the tag integrated circuit. This can be achieved by transmission of transmission of binary 0 and 1 in every symbol that is transmitted. This provides the necessary continuous energy to keep the tag integrated circuit turned on. This approach is referred as Pulse interval encoding PIE. A single symbol is shown in the figure 3-2.

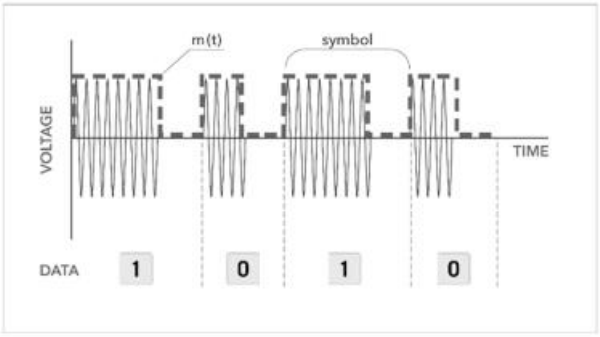

Figure 3-2 *Pulse Interval Encoding approach* ***[15]***

Tag, on receiving the transmitted high frequency signal from the reader, converts it to DC voltage with the rectifier circuit and turns on the fabricated integrated circuit. Once the integrated circuit has enough power to turn itself on, it demodulates the signal using the envelop detection mechanism and decodes the signal. The signal transmitted from the tag over the uplink channel, also known as back scattered radio channel, is modulated using the impedance modulation. In Impedance modulation, the tag antenna is connected to different loads corresponding to binary 0 and 1s, resulting in variation of current in the antenna.

The reader receives the electromagnetic signal transmitted from the tag, demodulates and decodes the signed and sends it back to console for interpretation.

3.2 RFID Reader

The reader antenna is meant to build a connection between the propagating electromagnetic waves and electronic circuitry of the reader. The operating frequency or bandwidth, gain and directivity characterize antennas. High gain results in narrowing the beam width of the antennas and the most of the energy is concentrated in the main lobe of the antennas.

As the vector potentials takes account of the currents and electric fields, whose polarization can be controlled by using the current pattern within the radiating body of the antenna. Depending on the current path in the radiating body, the polarization can be forced to circular instead of linear.

In UHF range, reader antennas come in number of design specifications with high directivity and gain to increase the read range of the antennas. The tag antenna must be in the read range of the reader antenna. On the other hand, the reader antenna gain is linked to the size of the antenna. The higher the gain of the antennas, higher will be the directivity of the antennas and larger will be the size. Therefore, high directional antennas are not feasible for hand held application; instead, we use patch, half wave dipoles and helix antennas.

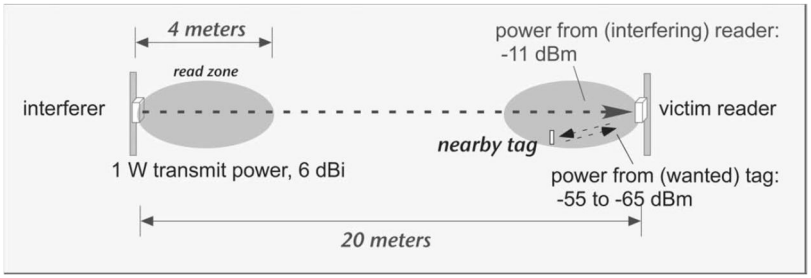

Figure 3-3** Interference between the antennas **[15]

Patch antenna is used in most of the stationary RFID readers. With the single dipole labels works with circular polarization, however, with the double dipole tags, the polarization is no more discriminating. A reader antenna is supposed to cover every tag in the read range zone. The readers may interfere with each other, which can cause the reader to screening, or blocking the direct paths, as the interference from the reader antenna could be much larger than the reflected signal from the tag. Figure 3-3 shows the mechanism for the interference from the other radios in the ISM band.

Near filed antennas are simple to construct with a limitation of small read range. However, when it comes to construct an antenna with read range comparable to the wavelength of the antenna radiation, it becomes difficult to construct having the resonant properties

of large loop antennas. One solution could be to use discrete or segmented loop with capacitive tuning.

The connectors and cables used for the antennas feeding introduced losses, however, provides the flexible and reliable attachment of cabling of the reader antenna and reader, and feasible site selection for the reader antenna. Thinner the cables are, more will be the loss introduced by them.

3.3 Power Transfer

In the passive UHF RFID tag, the tag-received power from the reader signal should exceed the threshold power level to turn on the integrated circuit of the tag for reading purpose, which is usually 10-30μW. However, much more power is need to write the data on the integrated chip [23]. However, in practical while considering the efficiency of the rectifier, the power needed to turn on the integrated circuit would become 30-100μW [15]. Therefore, the actual received power can be found by the Friis equation,

$$P_r = P_t G_t G_r (1 - |\Gamma_r|^2)(\frac{\lambda}{4\pi R})^2, \quad (3.1)$$

Where Γ_r is the reflection coefficient of the receiver antenna and involved the antenna impedance matching.

3.4 Project Motivation

Body Area Networks BANs, which is extension of the Personal Area Networks, which is used for communication of different devices or nodes, placed on human body. Wearable antennas are used for communication of the nodes and at the same to avoid any hindrance of the body. In the field of RFID, most of the work on the wearable technology is done on the wearable tag [24] [25] [26] and not much work is done on the RFID wearable antenna. The wearable reader antennas are designed on non-flexible substrates, which hinders the body moment.

In this thesis, two wearable antennas for the RFID reader application has been designed. The type of antenna selected for the application are the SRR and the slotted patch antenna tuned at a frequency of 860 MHz. To keep the antenna wearable, flexible materials are selected for the radiating element of the antenna and the substrate. Ethylene Propylene Diene Monomer (M-class) rubber *EPDM* is used as the substrate having permittivity of 1.26 and the loss tangent is 0.007 of various thickness of 4mm and 3mm. On the other hand, the nickel and copper plated conductive textile with sheet resistance of 0.16Ω/square. The antenna should be mounted on the working hand gloves; therefore, it should be compact and comparable to the size of the hand. The performance of both the

antennas are measure in free space and in the close vicinity of the body. The measurements included the bending results of antennas.

Both the antennas showed quiet much difference between the simulated and measured free results that might occurred due to the fabrication inaccuracies. Some frequency shifting is also observed when compared to the simulation.

4. WEARABLE ANTENNAS TECHNOLOGY

This chapter emphasis on the wearable antenna, their importance and brief history. Sections describing the body area networks (BAN), impact of body area networks and current development on the wearable antennas.

Body Area Networks

Body area network is a communication standard streamlined for low powered gadgets and optimized to operate in, on or around the human body to serve for various applications including medics, customer/personal excitement and other [27].

A body area network consists of different hubs connected to various parts of body. These hubs are in charge of communicating with each other and transmitting the data to remote server wirelessly [27]. A hub comprises of a sensor for getting real time data, an actuator to deliver the response of the BAN system, and Personal Digital Assistant (PDA) for monitoring purpose. The most sophisticated and complex part of a BAN system is the sensor, which is capable of data stockpiling over the period and an antenna for reception and transmission of the gathered information [28]. In general, a specifically designed antenna for the BAN networks should be:

1. Miniaturized and lightweight
2. Flexible, foldable and should retain their shape
3. Radiate away from body
4. Stability in characteristics in the human body region
5. Cost Effective
6. Robust

In the start of twentieth century, with the development of electro-textiles, the researchers have built the wearable antennas that are flexible enough to allow the normal movement of the body.

4.1 Wearable Antennas

Researchers has developed a number of wearable antennas of different types, including the patch antennas and split ring resonators. Different type of patch antennas were made including T- slotted, U-slotted and E-slotted for the BAN networks. In the end of the ninetieth century, the wearable antenna technology managed to captivate the attention of the researchers and for the first time in 2001, researcher managed to use the fabric as antenna substrate to make wearable antennas. The very first research work on a dual band planar wearable antenna tuned at 2.4 GHz design for Global System for Mobile Communications (GSM) and Bluetooth applications was published in year 1999 [29]. The antenna was miniaturized and dual band characteristic was achieved by inserting a U shaped

slot in the radiating element of the patch antenna with ground plane to minimize the influence of the body electric properties on antenna performance. The design was such that it can be mounted on the sleeves of the human body. Although, the antenna was designed on a rigid non-flexible substrate, but the compactness of the antenna made it possible to be mounted on the human body.

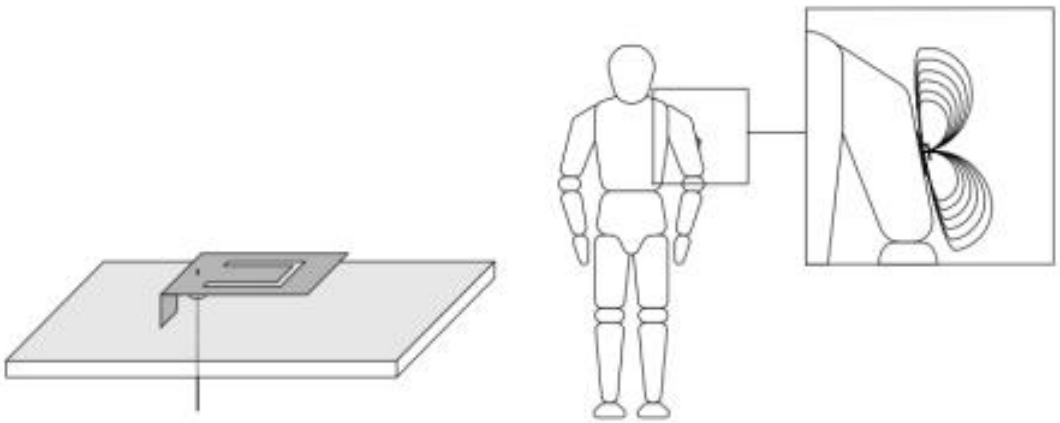

Figure 4-1 *Wearable antenna designed for human body (a) Structure (b) antenna mounted on human arm*

After this step forward in the wearable antenna technology, researchers started working on the upcoming technology by designing the antenna with different substrates and conductive materials. In 2001, an antenna was designed using the fabric as substrate, which made it possible to comfortability in wearing the antenna on human body. The development in these type of antennas using the fabric gave rise to a new domain, today known as textile antennas. Furthermore, another wearable inverted F antenna was introduced—UMTS 2.1 GHz and 2.4 GHz WLAN bands—using flexible substrates. These antennas were majorly for the smart clothing purpose, enabling the mountable devices to communicate with the body away devices [30]. Later, in 2003, fleece fabric antenna tuned at 2.45GHz frequency was introduced [31]and the work on effects of wearable micro-strip antenna bending was also published in the same year [32].

From the year 2003-07, different type of substrates and conductive fabrics, for example electro-textiles, were used to build various type of antennas for safety measure and for the military applications. Electro-textiles has properties including better conductivity and less resistivity, which resulted in better performance of the wearable antennas. Furthermore, embroidered antennas were also introduced to with the invention of the conductive threads.

As the wearable antennas operates proximity the human body, it became important to study the impact of the human body electrical properties on the design of the antennas. In 2004, a research paper “Wearable antennas in the vicinity of the human body”, represented the detailed account of the antenna performance near human body [33]. Although,

different human body parts exhibits different properties due to thickness of the Muscle and different layers of Fat, Muscle and skin, hence, the paper analyzed the upper part of the human body including the arms and the chest.

As discussed in the section 1, the antenna selection is of the core importance, when it comes to wearable antennas. For this project, the antennas is meant to be mounted on the working hand gloves, therefore, the antennas should be narrow band (2MHz), linearly polarized, compact in size to fit on the hand gloves and have minimum effect of bending, flexible, stable characteristics in human body proximity. Furthermore, the antenna should be less sensitive toward substrate thickness as in this project the substrate is the gloves that has variable thickness and air gaps between the hand and the gloves, furthermore, the antenna read range should be up to one meter is expected. Keeping these in the mind two types of antennas were best fitting the application; Spilt Ring Resonator and Slotted Patch antenna. Here are some of the literature review about both of the antennas is discussed.

Split Ring Resonator Antenna:

In 1999, Pendry et al invented a new structure fundamentally for building the metamaterials and named it as Split Ring Resonator (SRR) [34]. As the exhibits the negative permittivity and permeability, it was initially purposed only for building metamaterials and it has been used in sonic and optical applications [35]. The primary structure used in [34], is shown in the figure 4-2. Initially work includes the building of the metamaterials with concentric circular split rings resonators. In 2013, Pedro J. Castro studied the effect of different slit widths on the resonance of the split rings [36].

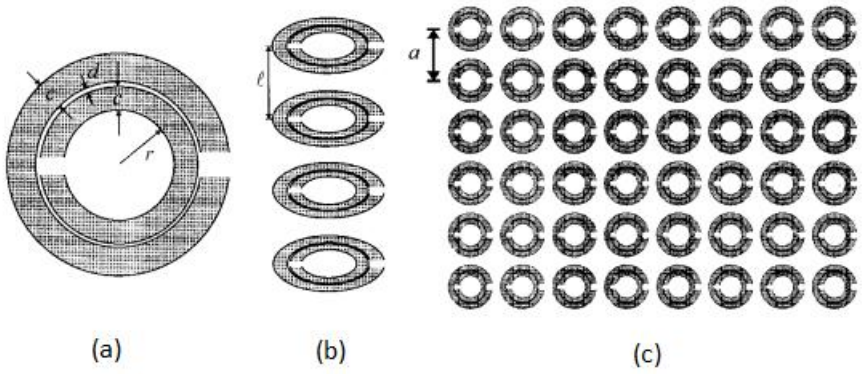

Figure 4-2 *Basic building block of Metamaterials--Split Ring Resonator (b) Stacking sequence of SRR (c) Plain view of the SRR structure in a square cubic array* ***[34]***

Later experimentation done on the metamaterials resulted in more structure of the building blocks of metamaterials. In July 2008, Jiangfeng Zhou studied the U shaped SRR and concluded that higher order of modes for excitation were found for both electric and magnetic resonance [37]. In 2013, Rajni studies the square geometry of the split ring resonators [38].

In 2008, X. Yang studied implemented an antenna using individual SRR element and studied the properties of the antenna. The structure of a single SRR element used, is shown in the figure 4-3.

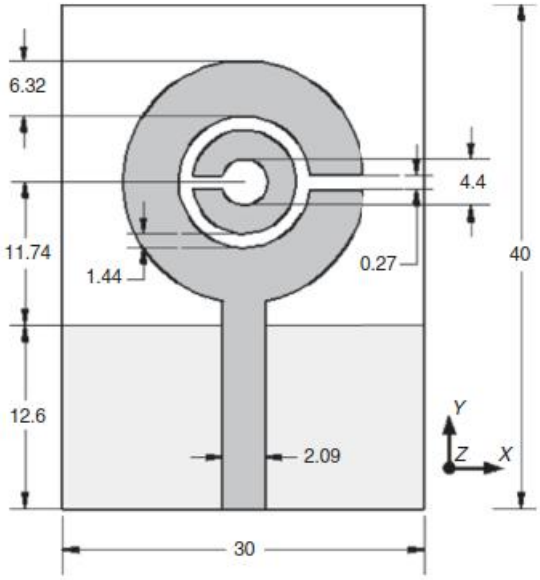

Figure 4-3 *Structure of individual SRR ultra wide band antenna*

Split Ring Resonator antennas has the unique property of resonating at a frequency with wavelength much longer compared to the antenna dimensions which make it miniaturized at the same performance and properties. The resonance frequency of the SRR antennas is a function of the inductive and capacitive behavior of different conductive parts of the antenna and gaps between the two rings. In general, these capacitive and inductive behavior of the antenna can be varied using the parameters a,b,c,d, r, angle between the splits and the slit widths. Extensive work has been done to study the behavior of the parameters, input impedance and the resonance frequency [39]. Abdolsakoor in 2013, studied the impact of the angle between ring slits on the resonance frequency of a single split ring resonator antenna [40]. At first resonance frequency, the behavior of the SRR antenna is similar to that of the dipole antenna, which can be modelled as series LC circuit with the resonant frequency given by,

$$\omega_0 = \sqrt{\frac{2}{\pi r_0 L C_{pul}}}, \tag{3.1}$$

Where, C_{pul}, L and $r_o$is capacitance per unit length between the rings and the slits, total inductance and average radius of SRR antenna [41].

One of the antenna purposed in this project is the circular split ring resonator antenna because of the fact that, it can resonate at much lower frequency as compared to its dimensions. The surface area of the antenna is kept small intentionally to minimize the

impact of human body electrical properties. Designing and implementation of the SRR antenna will be discussed later in section 5.

Slotted Patch Antenna:

Although, the invention of the micro-strip patch antennas can be traced down in 1953, however, the micro-strip patch antenna received remarkable attention of the researcher in 1970s [10]. The micro-strip antennas often are also known as *patch antennas*. A typical patch antenna comprises of a radiating patch, a substrate and the ground plane, shaoen int the figure 4-4 [10]. The ground plane is an important feature for patch antennas, when it comes to wearable antenna technology, as it can reduce the influence of body electrical properties on the antenna designing and performance. the radiating element of the patch antenna and the feed line is usually attached on the top of the substrate. Usually the radiating element of the patch antenna is square, rectangular, circular, elliptical or in some other regular shape, but can be miniaturized by inserting a slot in the radiating element. The shape of the slot may also vary depending upon the designing of the antenna; it may be U shaped, L shaped or T shaped.

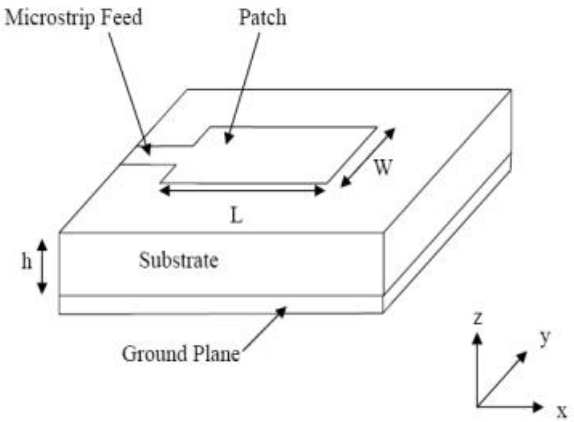

Figure 4-4 *Rectangular patch antenna*

For the first time in 2004, circularly polarized patch antenna was designed using textile for wearable applications [42]. The antenna used a single inset line to feed the antenna and truncated edges were used to achieve the circular polarization. Dual band rectangular patch wearable patch antenna was implemented using Jeans as the substrate material in [43]. Another design used for wearable RFID tag is purposed in [44] using the T slot for miniaturization of the patch antenna as shown in the figure 4-5. Electro-textile material was used as the ground and the radiating element and the substrate of the antenna was EPDM material.

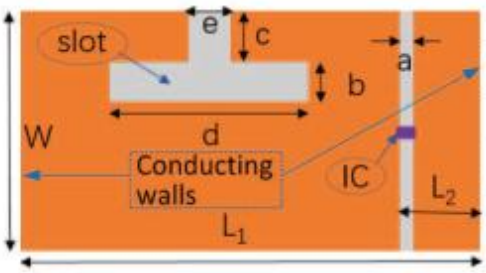

L1	L2	W
63.7	10.1	29.8
a	b	c
2	5	7.68
d	e	t
27.1	5	2

Figure 4-5 *Design of a slotted patch antenna for RFID tag application*

The design techniques used in this project is similar as discussed in [44], with minor amendments in the design and will be discussed later in the chapter 5.

Need of Improvements in wearable antennas:

The literature review of the Split Ring Resonator antenna shows many design aspects, however still some improvements can be made:

1. Most of the research done on the Split ring resonator is directed towards for building the meta-materials. However, some research also includes the behavior of single split ring resonator antenna.
2. Compact Slotted Patch antenna are developed mostly for the tags, however, some work is also done on designing the antenna with flexible material. Conductive textile materials can be used to build an antenna for RFID reader.
3. Single element SRR antenna is mostly designed with copper material and can be implemented as single element with the conductive textile for wearable applications.
4. Effect of different thickness of the substrate can be studied along with bending analysis on
5. Effect of bending on SRR and the slotted patch antenna and near body analysis can be studied for effective designing.

5. SIMULATION OF WEARABLE ANTENNAS

This chapter discusses the designing of both SRR and the slotted patch antenna on the EPDM substrate and using the electro textile. The simulation software used for designing the antennas is the Ansoft High Frequency Structure Software (ANSYS HFSS) 2017. HFSS utilizes numerous state of the art solver techniques based on finite element integral and differential equations and other methods to resolve a variety of extensive radio frequency and microwave problems [45].

Due to continuous motion of the human hand with frequency dependent permittivity, it becomes difficult to tune the antenna on one frequency consistently as the bending have effect on the tuned frequency. There are two reasons for this problem, To minimize the bending effect the antenna is mounted on the back of the hand. In addition to this, the antenna surface area in case of SRR was kept as less as possible to minimize the interaction between the antenna and the human tissues. The reason to construct the slotted patch antenna is to compare the results of the SRR antenna and study the difference in performance of both the antennas.

5.1 Human Hand Model

As the antenna is to be mounted on the working hand gloves, therefore, a simplified body model having realistic permittivity and conductivity model was established for the simulation of the antenna. The thickness of different layers of hand including skin, muscle, fat and bone are shown in the table 5.1. The conductivity and permittivity of these human tissues were taken from [46]. The permittivity is shown in the figure 2-1 and figure 2-2.

Table 5-1. *Thickness of human tissues*

Body Model	**Thickness (mm)**	**Length (mm)**	**Width (mm)**
Dry Skin	2mm	280mm	110mm
Muscle	2mm	280mm	110mm
Fat	2mm	280mm	110mm
Bone	1cm	280mm	110mm

The different layers were stacked one on other to make a flat human body model with dimensions in accordance to the table 5-1, whereas, figure 5-1 shows the flat human model of the antenna.

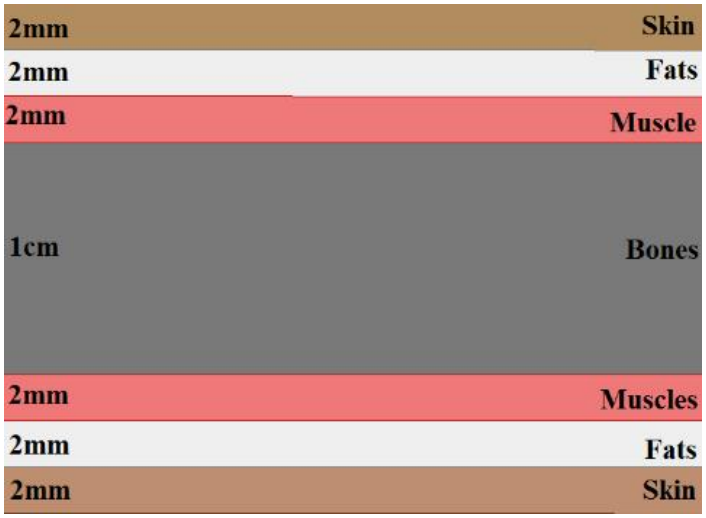

Figure 5-1 *Human body model used for the simulations*

Permittivity of Human Body

Unlike most of the materials, permittivity of the human body is not constant rather it becomes frequency dependent. This is due the reason that the human body acts as a lossy material for the electromagnetic waves. In addition to that, human body comprises of 75% of the water, due to which it effects the radiation properties of the antenna. The dielectric properties of human body at radio frequencies and microwave frequencies has been studied in [47]. The permittivity of human body tissues like dry skin, Fat, Muscle and Bone are shown in the figure 5-2.

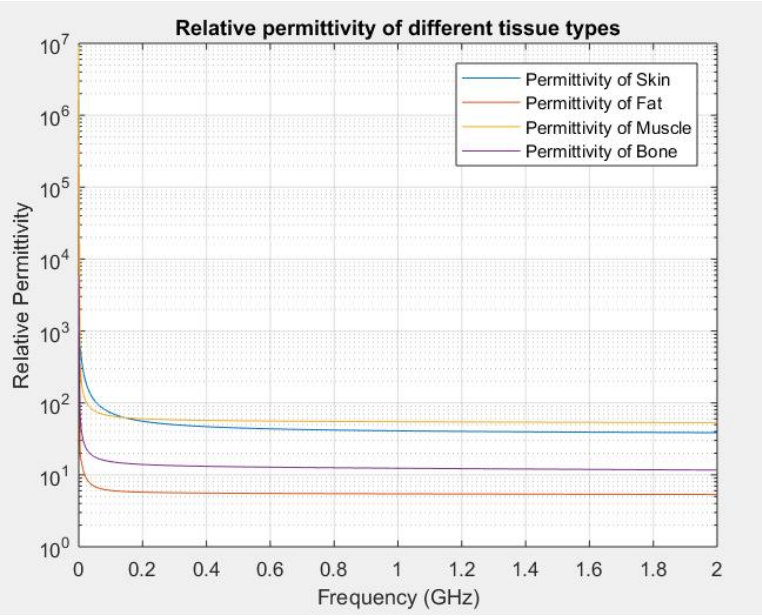

Figure 5-2 *Relative permittivity of different tissue types*

The figure -2 shows the human body model used for the simulation. It contains layers of skin, Fat, muscle and Bone.

The conductivity of Bone, Muscle, Fat and skin is shown in Figure 5-2(a). Like permittivity, the conductivity of the human body is also the function of frequency and has a direct relation.

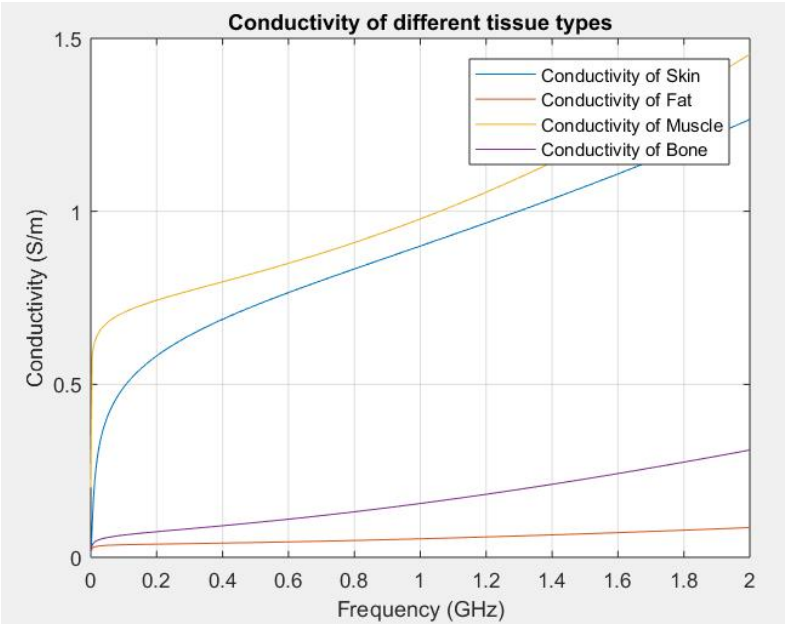

Figure 5-2(a) *Conductivity of different tissue types*

The loss tangent of different tissue types are shown in the figure 5-2(b), which includes the contribution from both the polarization and conductivity.

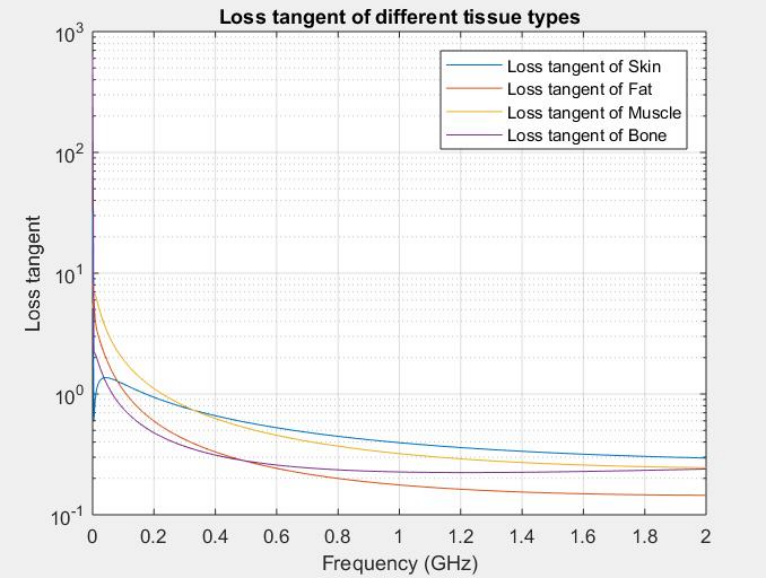

Figure 5-2(b) *Loss tangent of different tissue types*

A multi-dispersion model was used to predict the frequency dependent relative permittivity of different body tissues [48]. In the model, the frequency range is characterized by the dispersion region and the analysis leads to the insight of the relationship between the molecular parameter of the biological materials and the dielectric. According to the model, the dielectric spectrum of the tissue is divided into high, medium and low frequencies. The model expressed the complex permittivity of the tissue as a function of the frequency as

$$\hat{\varepsilon}(\omega) = \varepsilon_{\infty} + \Sigma \frac{\varepsilon_s - \varepsilon_{\infty}}{1+(j\omega\tau_n)^{(1-\alpha n)}} + \frac{\sigma_i}{j\omega\varepsilon_o}, \qquad (5.1)$$

where the ε_{∞} and ε_s is the permittivity when $\omega\tau \gg 1$ and $\omega\tau \ll 1$ respectively and the $j^2=-1$. In the equation 5.1, τ, σ_i, and ε_o is the time constant, the static ionic conductivity, and the permittivity of vacuum and α is the distribution parameters which measure the variation in the magnitude of dispersion $\Delta\varepsilon = \varepsilon_s - \varepsilon_{\infty}$.

5.2 SRR Antenna

The geometry of the SRR antenna is shown in the Figure 5-3. The material selected as substrate is the *EPDM* material having thickness of 3 mm and the dielectric constant 1.26 and the lost tangent 0.007. The SRR resonates at a frequency of 860 MHz. The thickness of the substrate is 3mm which indicates the antenna will have narrow bandwidth which also requirement of the application. The inner ring helps to impedance matching to 50Ω. The antenna can be tuned to a certain frequency by varying different parameters of as mentioned in the Figure 5-3. The antenna is optimized to give a maximum read range, when mounted on the working hand gloves. This section focuses on the designing of the SRR antenna using variations in different parameters of the antenna.

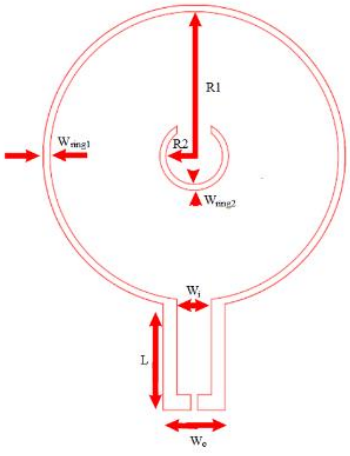

Figure 5-3 *Split ring resonator antenna geometry*

Effect of outer ring radius R_1 on return loss

The figure 5-4 shows, the variations in the radius of outer split ring and its effect on the resonance frequency and the magnitude of the return loss. It can be seen that with the

increase in the radius of the outer ring—***R_1*** *labelled in the figure 5-3*—results in shift of the resonance frequency to higher frequencies. The magnitude of the return loss tends to decrease with increase in the radius, which is not desirable. As shown, at 44mm outer radius, the return loss at 860 MHz frequency is approximately -12dB and can be further improved by adjusting other parameters discussed in this section.

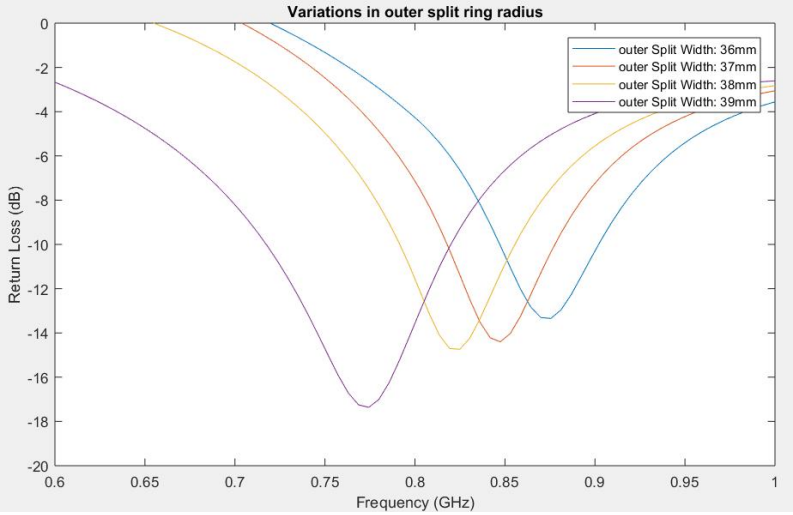

Figure 5-4 *Variations of return loss with radius of outer split ring*

Impact of split outer ring width W_{ring1} on return loss

The figure 5-5 shows the return loss variations with different widths of outer split ring. It can be seen that the return loss of the antenna is promising at 4mm outer ring width and further decreases at a width of 8mm and further increase in the variation does not have significant impact on the return loss.

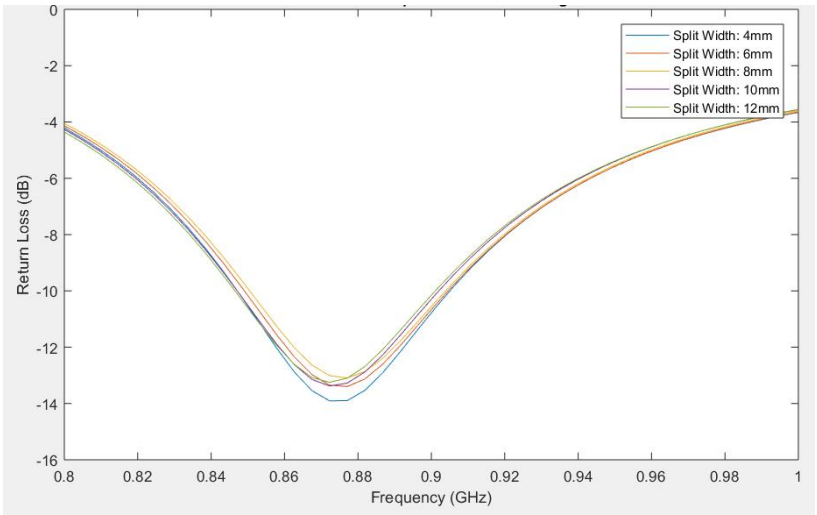

Figure 5-5 *Variation in width of outer split ring*

Impact of split width of outer ring W_i on return loss

Figure 5-6 shows the variation in the split width W_1 of the outer ring labeled in the figure 5-3. It is significant from the figure that shorter the width of the split ring is, better will be the return loss of the antenna.

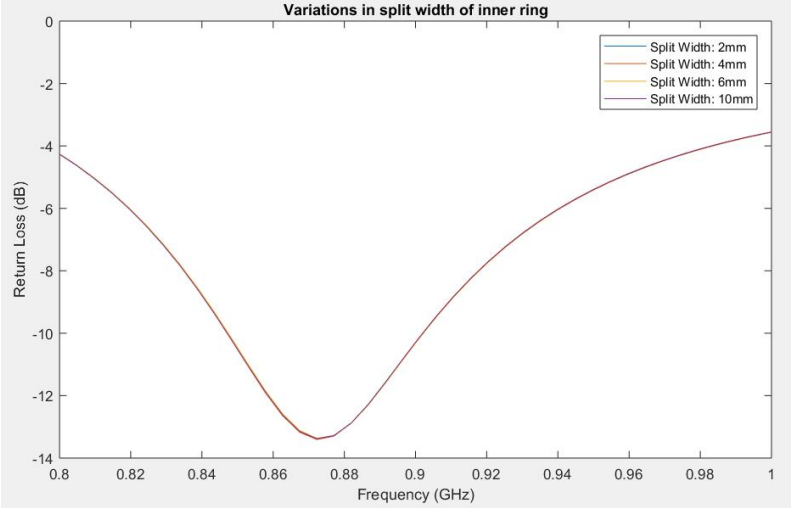

Figure 5-6 *Variations in split width of outer ring*

Impact of width of inner split ring W_2 on return loss

It can be seen from the figure 5-7, that the magnitude of the return loss decreases with the increase in the width of the inner ring until 29mm. However, when the width is further increased the return loss tends to increase. Therefore, the 29mm of thickness gives the optimum value for the SRR designing.

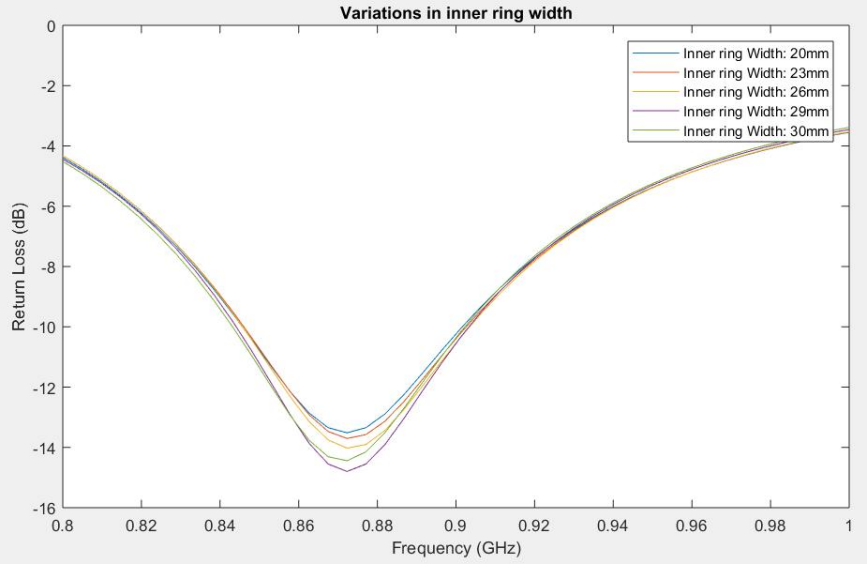

Figure 5-7 *Variations in the width of inner split ring*

Impact of split width of inner ring on return loss

According to the simulation, the split width of the inner ring has a inverse relation with the magnitude of the return loss. Lesser the width of the split better is the return loss of the antenna as shown in the figure 5-8.

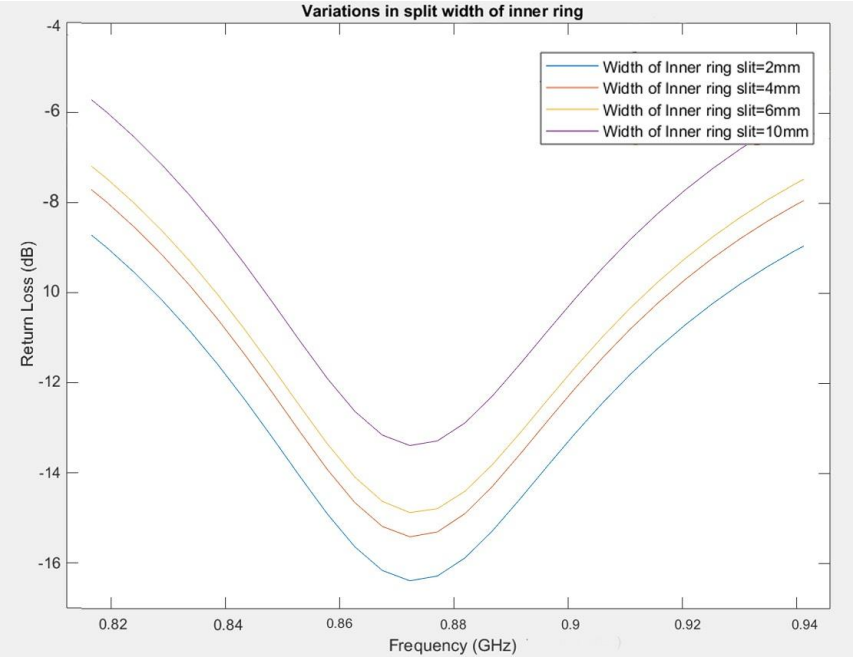

Figure 5-8 *Variations in the split width of inner ring*

Dimensions of the SRR antenna:

SRR antenna with dimensions listed in the table 5-2, resonates a frequency of 860 MHz frequency.

Table 5-2 *Dimension of the SRR antenna*

Dimension of SRR antenna	Length in mm
Radius of outer split ring	44mm
Width of outer split ring	2mm
Split width of outer ring	10mm
Inner ring radius	8.746mm
Width of inner split ring	1.254mm
Split width of inner ring	10mm
Length of feed line	32.3mm
Width of the feed line	4mm

Return Loss of the SRR antenna:

Figure 5-9 shows the return loss of the antenna at the 860MHz frequency. The bandwidth of the SRR antenna 50MHz (850-900MHz)

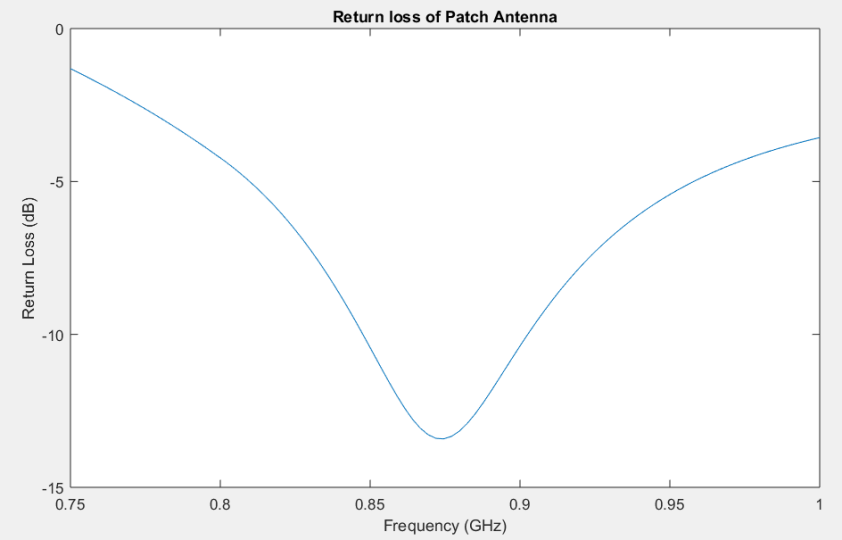

Figure 5-9 *Return loss of Split Ring Resonator Antenna*

3D Radiation Pattern:

The 3D radiation pattern of the antenna at 860MHz frequency is shown in the figure 5-10. The SRR antenna has a simulated gain of -2.88dB at 860 MHz frequency and is the main beam is directed in the positive z direction.

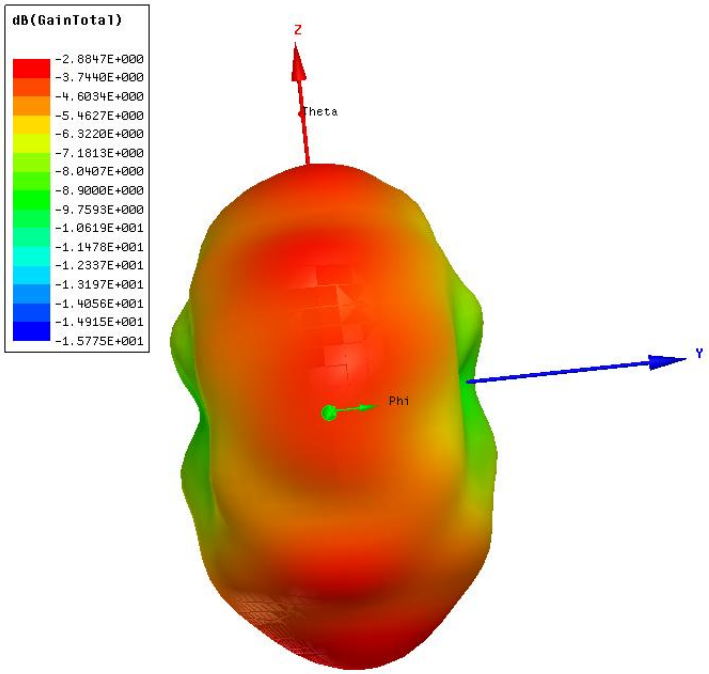

Figure 5-10 *3D radiation pattern of SRR antenna at 860MHz frequency*

Current Distribution on the Surface of the SRR antenna:

Figure 5-11 shows the current distribution on the surface of the SRR antenna at 860MHz frequency with different phases.

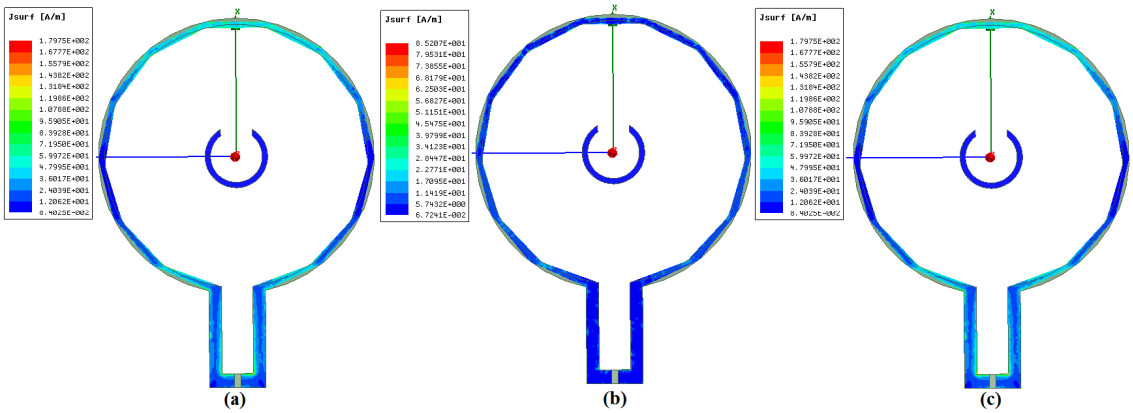

Figure 5-11 *Current distribution on the surface of SRR antenna (a)0° (b)90° (c)180°*

5.3 Slotted Patch Antenna

The geometry of the slotted patch antenna is shown in the Figure 5-12. The material selected as substrate is the *EPDM* material having thickness of 4 mm and the dielectric constant 1.26 and the lost tangent 0.0007. The slotted patch antenna resonates at a frequency of 860 MHz. The thickness of the substrate is 4mm, which indicates the antenna will have narrow bandwidth, which is also requirement of the application. The antenna can be tuned to a certain frequency by varying different parameters of as mentioned in the Figure 5-12. The antenna is optimized to give a maximum read range, when mounted on the working hand gloves.

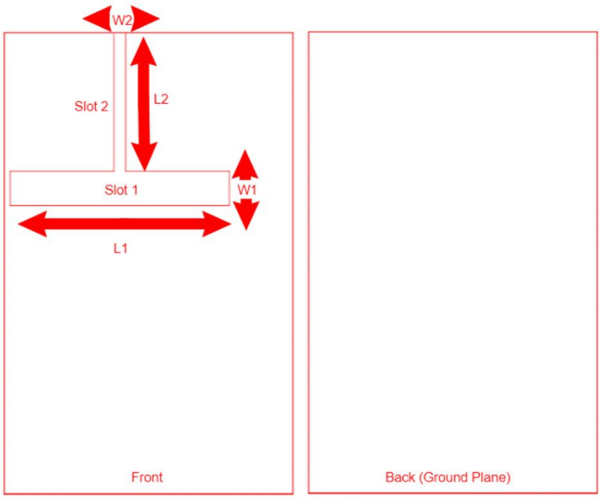

Figure 5-12 *Geometry of the slotted patch antenna (a) Front (b) Back (Ground Plane)*

As the largest dimensions of the antenna is constraint by the size of the hand, therefore for this reason, the length and width of the antenna is kept such that is should not exceed the size of the palm. The length and width of the antenna is 80mm and 50mm respectively and the slot dimensions are adjusted such that the antenna should resonate at 860 MHz frequency. This section focuses on the designing of the slotted patch antenna and impact of different variation in the slot dimensions.

Impact of variation is slot1 on return loss:

According to the simulations, increase in the length L_1 of the slot 1 give better return loss and shift the resonance to higher frequencies as shown in the figure 5-13. Whereas, with the increase in the width of slot 1 from 32mm, the return loss increases in negative and at 34mm, the return loss gives the optimum results. However, further increase in the slot width decreases the return loss, which is not desirable. In addition to this, the antenna bandwidth is increased at the antenna with increased width of the slot W_1 as shown in the figure 5-14.

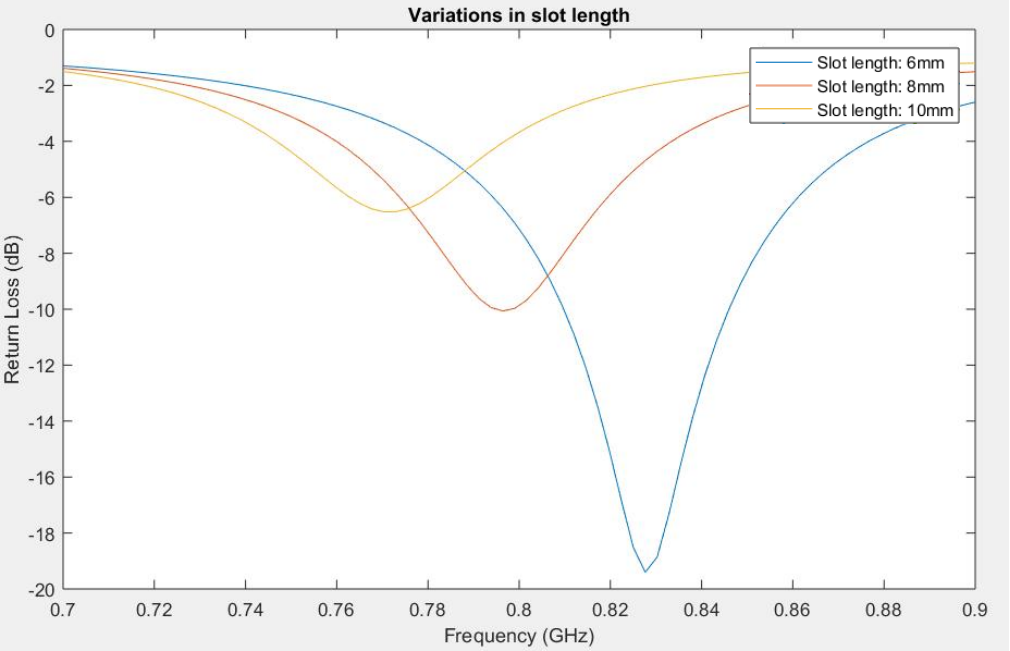

Figure 5-13 Variations in the length L_1 of slot 1

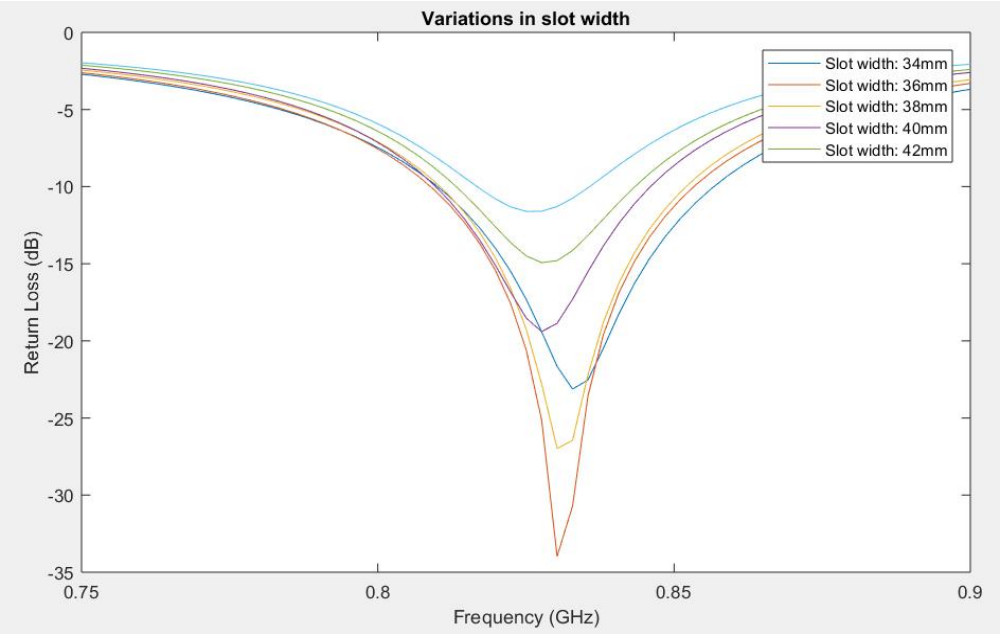

Figure 5-14 variations in the width $W_1$of slot1

Impact of Slot 2 dimensions on return loss

According to the simulations, increasing the length L_2 of the slot2 improves the return loss of the antenna and shifts the resonance to lower frequencies. At slot length 24mm, the antenna resonates at the desired frequency. Variations in the L_2 and the return loss is shown in the figure 5-15.

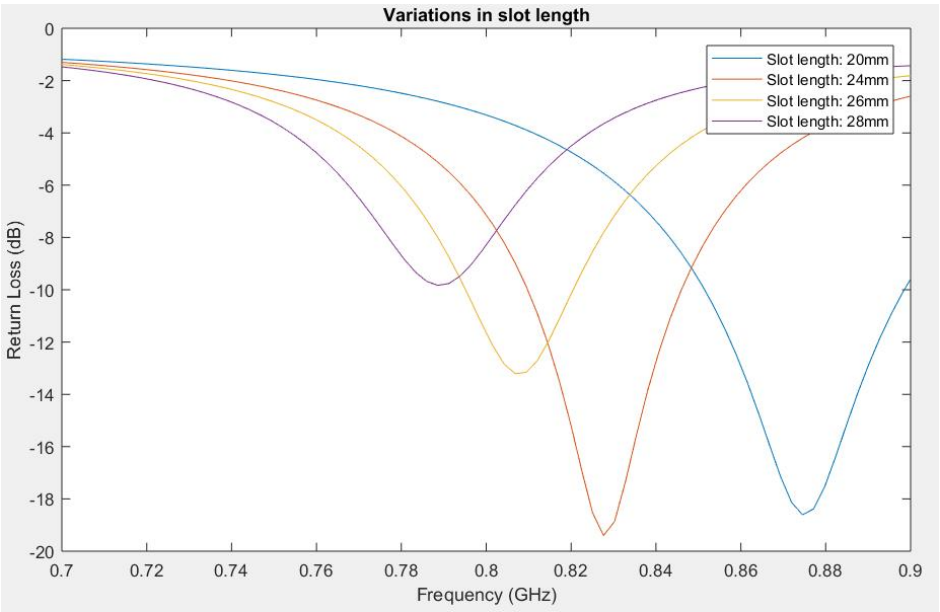

***Figure 5-15** Variations in length L_2 of slot2*

Variations in the width of the slot width W_2—shown in figure 5-16—is similar to the response of the variations in W_1. The increase in the slot width W_2 improves the return loss of the antenna and narrows the bandwidth of the antenna. At slot width 2mm, the

antenna return loss is approximately -25dB with a bandwidth of 30MHz starting from 860MHz to 890MHz.

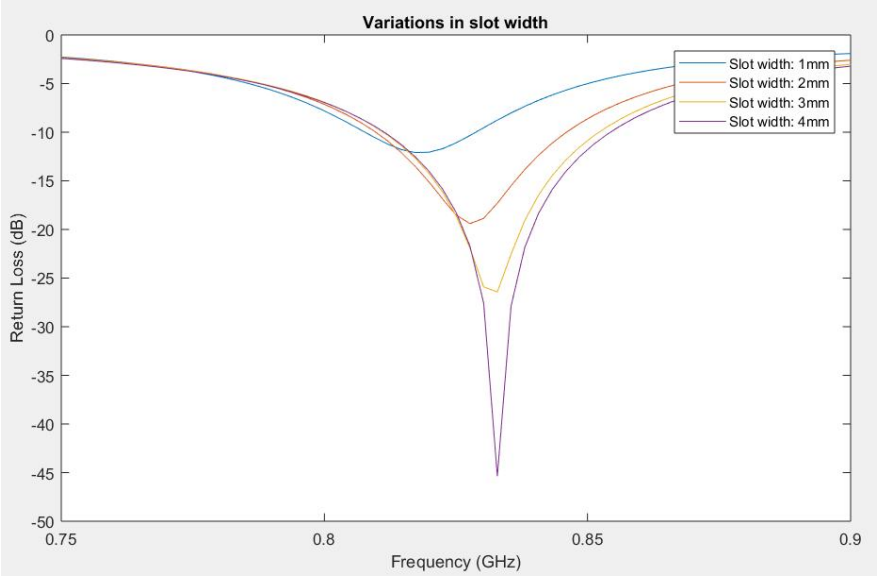

Figure 5-16 *Variation in the width W_2 of slot2*

Dimension of Slotted Patch antenna

Table 5-3 shows the slotted patch antenna dimension at which, the antenna resonates at 860 MHz frequency with acceptable return loss.

Table 5-3 *Dimension of the slotted patch antenna*

Dimension of Slotted Patch antenna	Length in mm
Length	80mm
Width	50mm
Length of slot1 L_1	38mm
Width of slot1 W_1	6mm
Length of slot2 L_2	21mm
Width of the slot2 W_2	2mm

Return Loss of the Slotted Patch Antenna

Figure 5-17 shows the return loss of the slotted patch antenna when mounted on the human body model is at the 860MHz frequency. The bandwidth of the slotted patch antenna is 40MHz (840-880MHz) and the return loss is -23dB

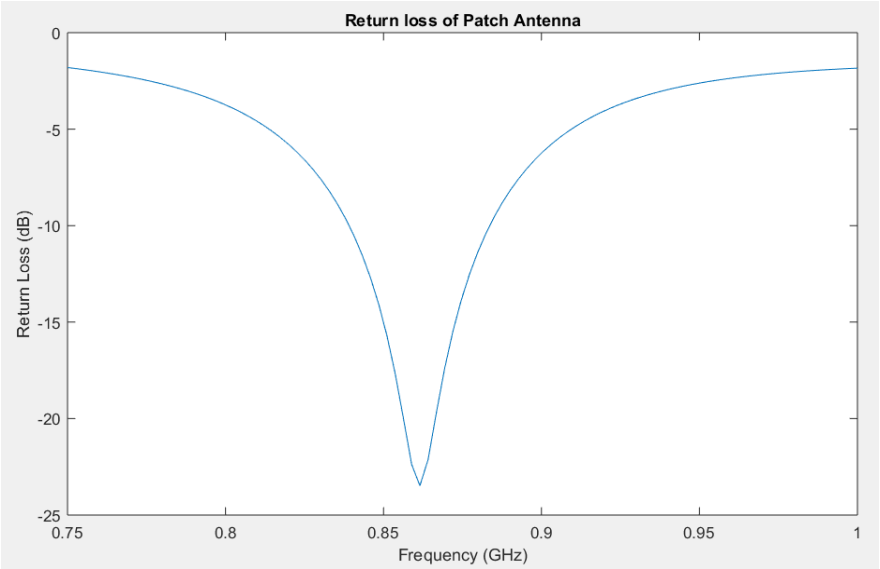

Figure 5-17 *Return loss of Slotted Patch Antenna on human body model*

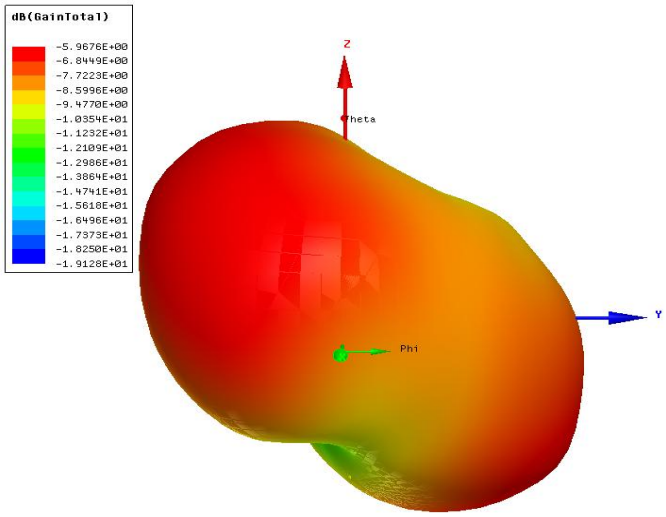

Figure 5-18 *3D Radiation pattern of Slotted Patch Antenna*

3D Radiation Pattern:

The 3D radiation pattern of the slotted patch antenna tuned at 860MHz frequency is shown in the figure 5-18. The SRR antenna has a simulated gain of -2.88dB at 860 MHz frequency and is the main beam is directed in the positive z direction.

Current distribution on the surface of the Patch:

Figure 5-19 shows the current distribution on the surface of the patch at 860MHz frequency with different phases.

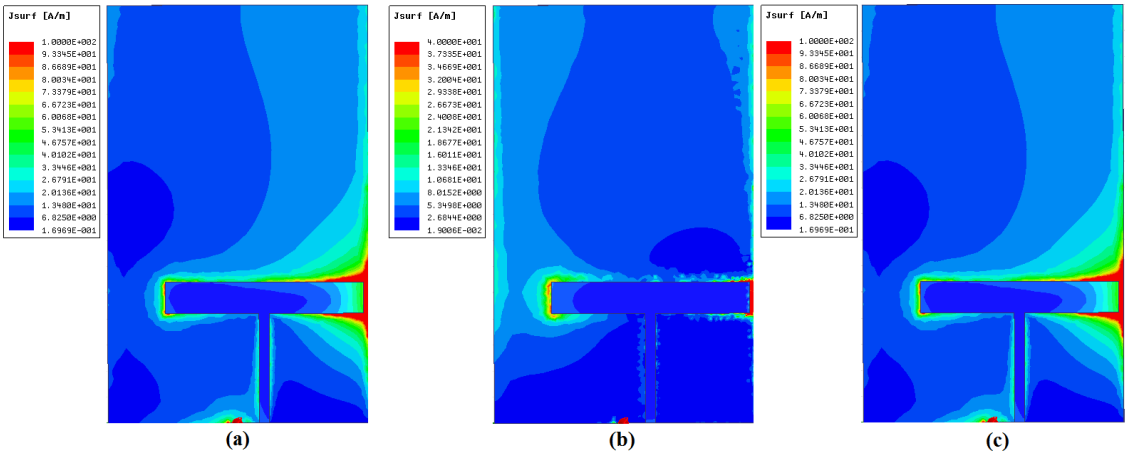

Figure 5-19 Current distribution on the surface of Slotted Patch Antenna (a)0° (b)90° (c)180°

6. FREE SPACE MEASUREMENTS

This chapter discusses the free space measurements of the both split ring resonator and slotted patch antenna. Measurements are taken using the Vector Network Analyzer (VNA) for the return loss measurements and the near field measurement device Satimo Starlab for radiation pattern measurements.

6.1 Free Space Measurement of SRR Antenna

The first antenna is designed and fabricated on EPDM substrate, which is lightweight, highly flexible, shock resistance and can be mounted on curve surfaces like hands [48]. On the other hand, the conductive element of the antenna is conductive fiber, which is also a lightweight, and flexible material with good conductivity makes the antenna suitable for the wear able applications. The figure 6-1 shows the free space measurement setup of the SRR antenna.

Figure 6-1 *Measurement Setup for using Vector Network Analyzer*

In free space measurement, the frequency is shifter to higher frequency because the permittivity of the free space is lower than the permittivity of the air. The figure 6-2 shows the comparison of the simulated and measured return loss of the SRR antenna in free space. However, the resonance frequency is shifted to lower frequencies due to inaccuracies in the fabrication of the antenna on the flexible substrate which can cause transform the geometry of the antenna. The measured bandwidth of the antenna is 35MHz (0.975GHz-1.01GHz).

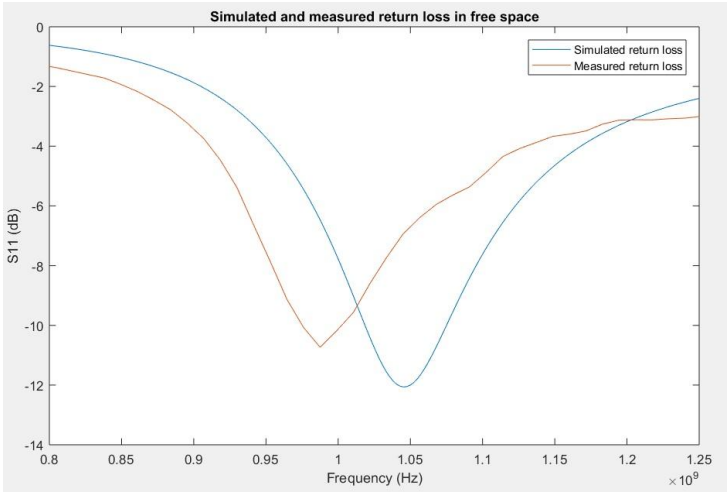

Figure 6-2 Measured and simulated return loss of the antenna in free space

Bending Measurements of the SRR antenna:

As the wearable antennas should be capable to bend in order to avoid the hindrance in the body movement. Therefore, it is necessary to study the effect of bending on the performance of the antenna. To study the bending effect, different bending shape with various radii were used to bend the antenna. The material of the bending surface used is such that it does not affect the surface current and the return loss of the antenna. To study the effect of bending, the antenna is bent in both xz-plane and yz-planes. A paper tape is used to hold the antenna and the cylinder together during the measurements. During the measurements, the performance of the antenna is analyzed by measuring the effect of bending on the return loss of the antenna. Figure 6-3 shows the bending of the antenna in different planes.

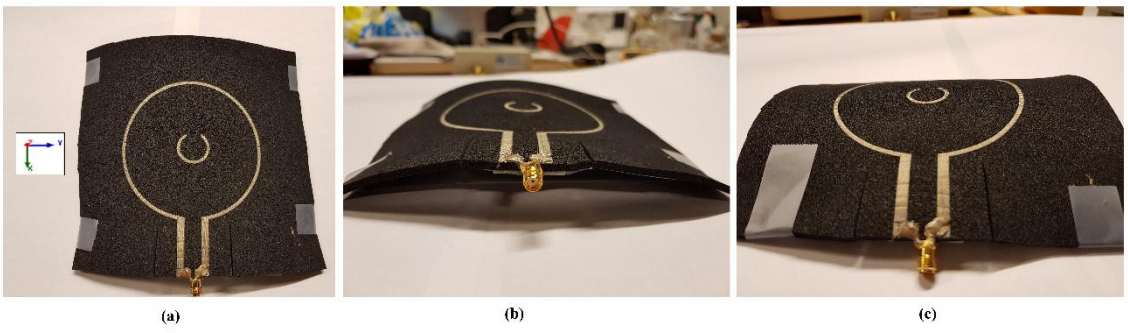

Figure 6-3 *Bending of the SRR antenna in different planes (a) SRR antenna (b) Bending in yz-plane (c) Bending in xz-plane*

Figure 6-4 and figure 6-5 represent a comparison between the measured return loss of the antenna in flat and bent state. As the bending of the antenna not only changes the geometry of the antenna but also changes the effective length of the antenna, which ultimately shifts the resonance frequency and the magnitude of the return loss. The figure 6-4 shows the bending in the xz-plane. It can be seen that the more bend is, the greater will be the shift in the resonance frequency and the return loss, lesser will be the bandwidth. One reason for this can be that the bending in xz-plane increases the ring split gaps which ultimate shifts the resonance frequency to lower frequencies.

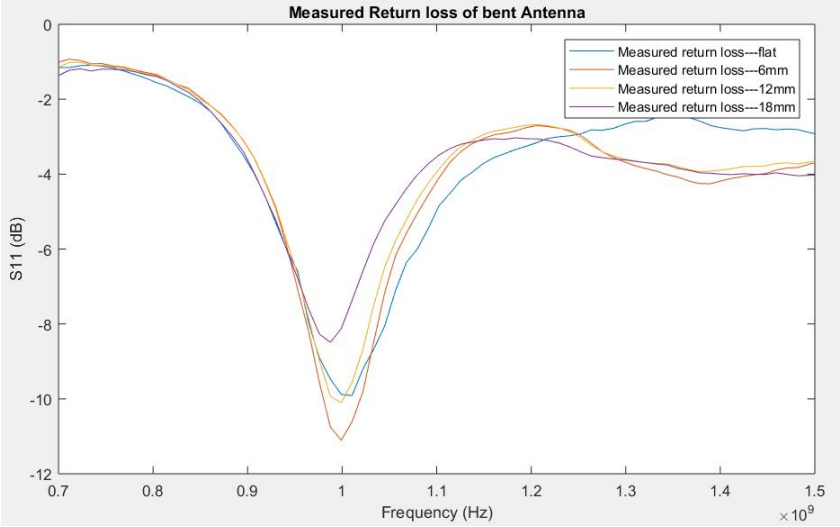

Figure 6-4 *Bending results of SRR antenna in xz plane*

The figure 6-5 shows the bending of the antenna in yz direction. In this picture, the bending of antenna shows opposite effect on the bending of the antenna. The resonance frequency is shifted to higher frequencies and with improved bandwidth and return loss.

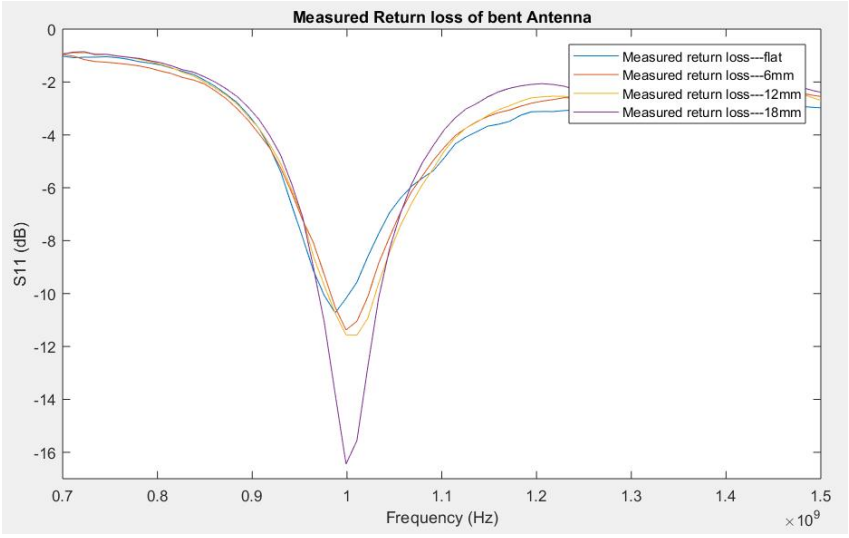

Figure 6-5 *Bending results of SRR antenna in yz-plane*

6.2 Free Space Measurements of Slotted Patch Antenna

The second antenna, slotted patch antenna is fabricated on EPDM material to compare the performance of both the antennas. The figure 6-6 shows the fabricated slotted patch antenna. The thickness of substrate is 4mm that is more as compared to the SRR antenna that is 3mm.

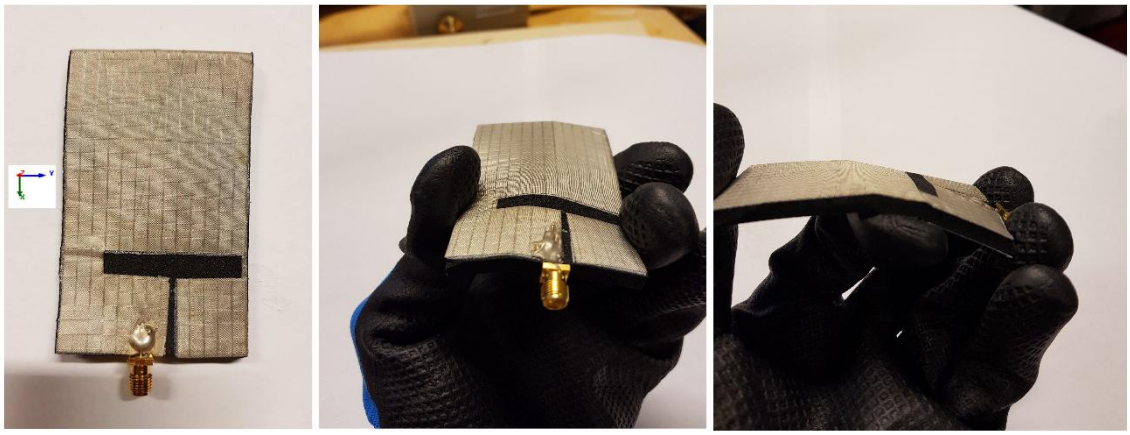

Figure 6-6 *(a) Slotted patch antenna (b) Bending in yz-plane (c) Bending in yz-plane*

The figure 6-7 represents a comparison between the measured and simulated return loss of the slotted patch antenna in free space. It can be seen that the resonance frequency is shifted to higher frequencies due to the inaccuracies in the fabrication process as two layers of the EPDM material were stacked on top of one another, which may contain uneven air gaps between them. The bandwidth of the antenna is 33MHz (847-880MHz).

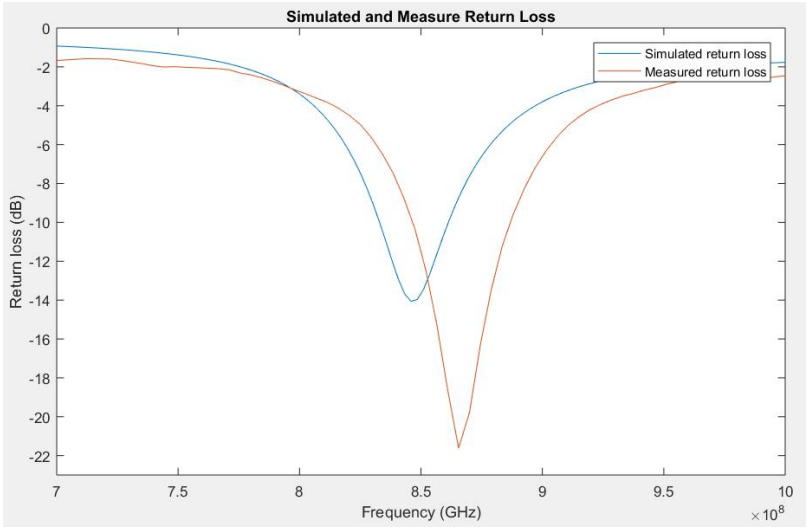

Figure 6-7 *Simulated and measured return loss of the slotted patch antenna*

Bending of Slotted Patch Antenna:

The bending is performed on the slotted patch antenna and its impact was studied on the antenna parameters. The figure 6-8 shows the antenna bending in xz-plane. It can be seen that the bending effect on the return loss of the antenna is negligible and it results in same bandwidth as in case of flat antenna.

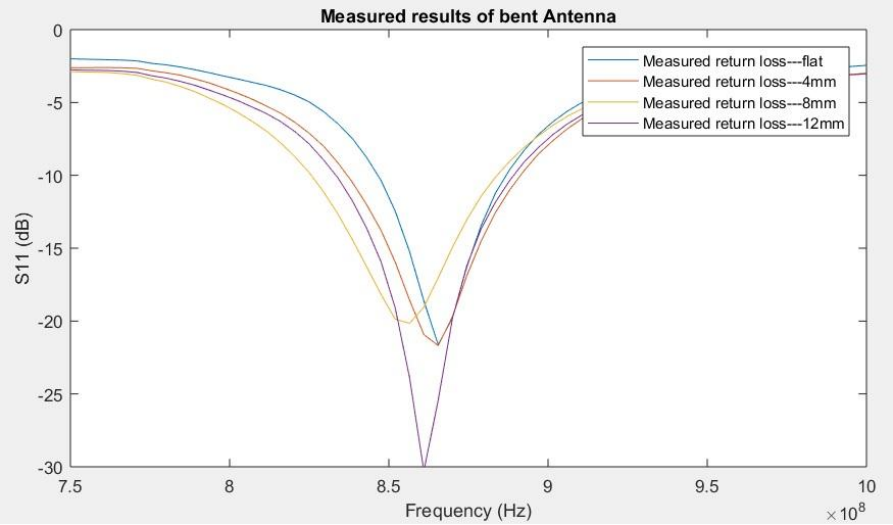

Figure 6-8 *bending of the slotted patch antenna in xz-plane*

The figure 6-9 show the bending results of the antenna in yz-plane. In this case, the resonance frequency is shifted to lower frequencies. The bandwidth of the antenna remains the same, however, the bandwidth is shifted from higher frequencies to lower frequencies but at the 860MHz frequency, the return loss of the antenna remains the same.

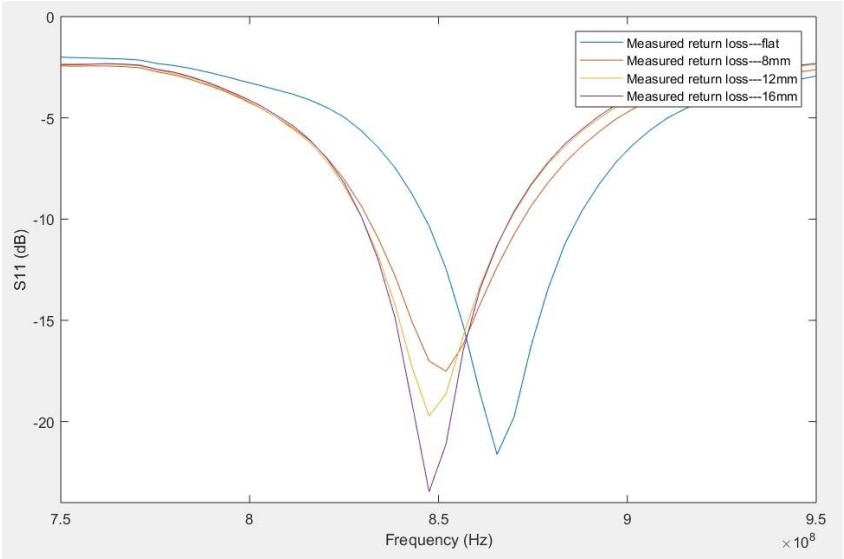

Figure 6-9 *Bending of the slotted patch antenna in yz-plane*

7. ON BODY MEASUREMENTS

This chapter elaborated the importance of measurements on the human hand. The human hand model is discussed in the section 5.1. The need of the on body measurements of the antenna arises as the human hand is not flat and wearable antenna may bend in different planes when mounted on the hand gloves. Therefore, the antenna designed for the human hand should be measured and checked in the real time environment.

7.1 On-body Measurement of SRR Antennas

Figure 7-1 shows the antenna mounted on the human hand.

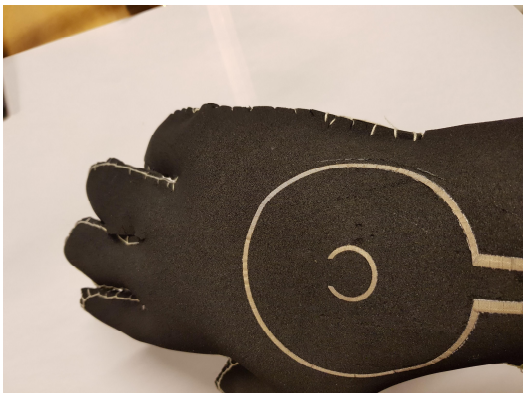

Figure 7-1 *SRR antenna mounted on hand*

The figure 7-2 shows the measurement of the antenna in the close vicinity of the human hand. The resonance frequency is shifted to higher frequency with the degraded return loss of the antenna due to the reason that the SRR antenna is a single layered antenna and does not have the ground plane which acts as an insulation between the body and the radiating element of the antenna. In addition, the body acts as a lossy material for the antenna, due to which, the antenna performance is greatly influenced in terms of antenna gain. . This results in decrease in the read range of the antenna. It is evident from the figure 6-2 and figure 7-2 that resonance frequency is shifted to lower frequency when antenna is moved from free space to close vicinity of the human hand. The bandwidth of the antenna, when mounted on the human body is 50MHz (890-940MHz) which is more as compared to the bandwidth measure in case of free space measurement 35MHz.

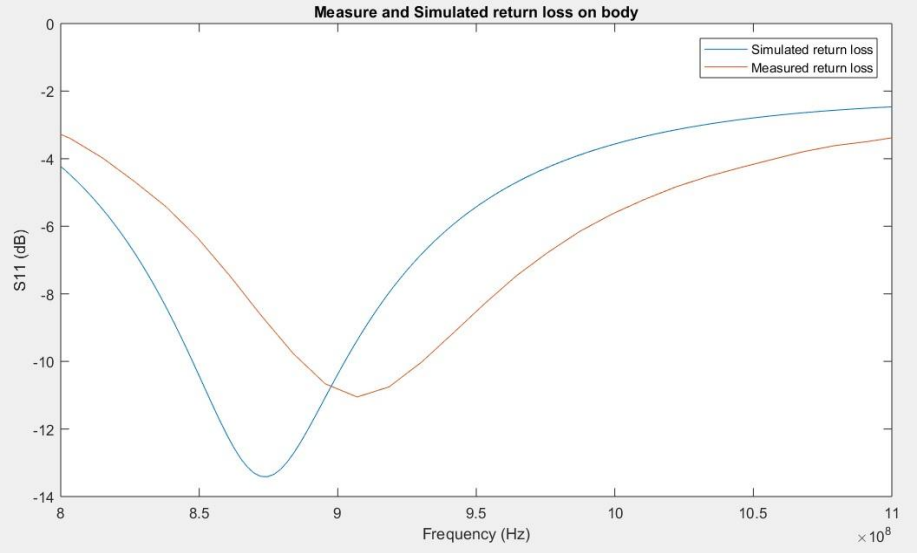

Figure 7-2 *Measured and simulated return loss of the SRR antenna*

Bending of SRR Antenna

Figure 7-3(b) and (c) shows the bending of the SRR antenna in yz and xz-planes respectively. The antenna is attached to the hand with transparent tape which has negligible effect on the antenna parameters.

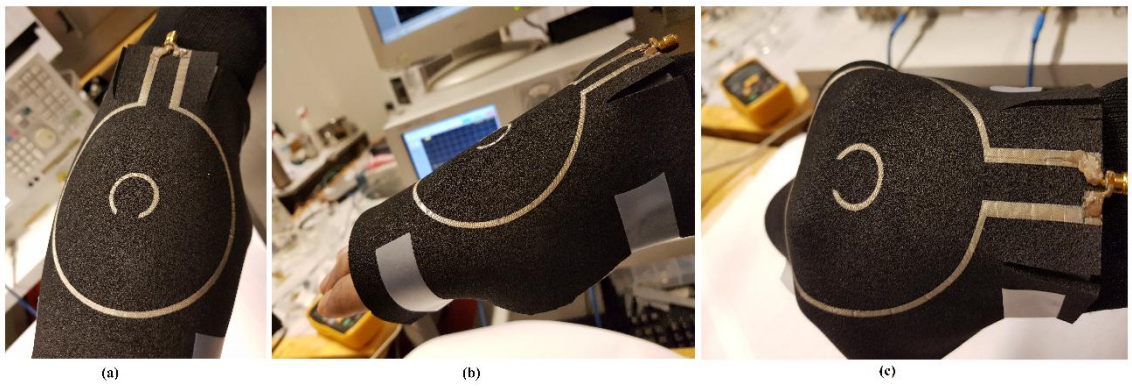

Figure 7-3 *(a) SRR antenna mounted on hand (b) Bending of the antenna in yz-plane (c) Bending of the antenna in xz-plane*

Figure 7-4(c) represents the bending of the SRR antenna in xz plane, when mounted on the hand gloves. It can be seen that the bending resulted in the shift of the resonance frequency to lower frequencies because of the reason that the bending effects the air gaps between the substrate and it also changes the effective surface area of the antenna interacting with the body, which in turns, effects the surface current of the antenna.

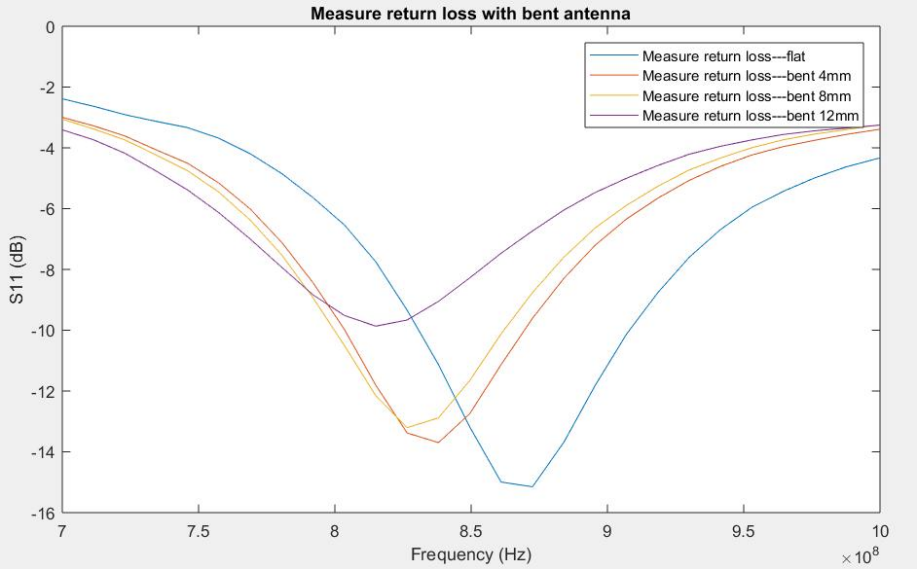

Figure 7-4 *Variation of return loss with antenna bending in xz-plane*

Figure 7-5 shows the antenna bending in yz plane on the human hand. It is evident that there is not significant effect on the resonance frequency of the antenna but it increases the magnitude of the return loss which results in decrease of the bandwidth of the antenna.

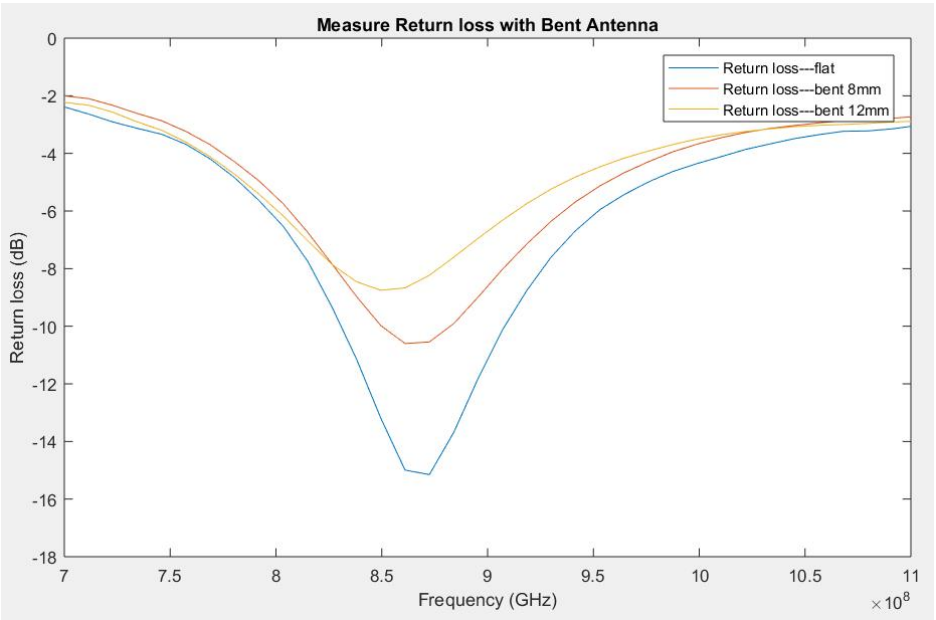

Figure 7-5*Variation of return loss with antenna bending in yz-plane*

7.2 On-body Measurement of Slotted Patch Antenna

The figure 7-6 shows the slotted patch antenna mounted on the human hand.

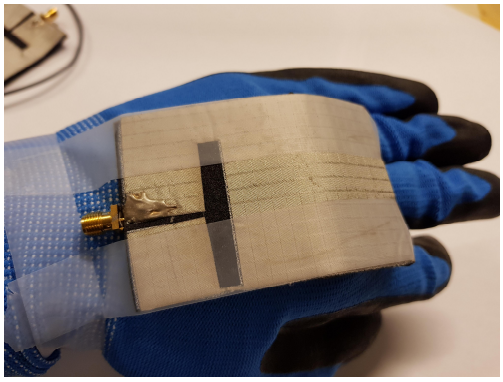

Figure 7-6 *Slotted patch antenna mounted on human hand*

As the slotted patch antenna possesses the ground plan, hence they are less effected from the human body properties. Therefore, their resonance frequencies remain close to as measure in the air. The figure 7-7 represents the measured and the simulated return loss of the slotted patch antenna.

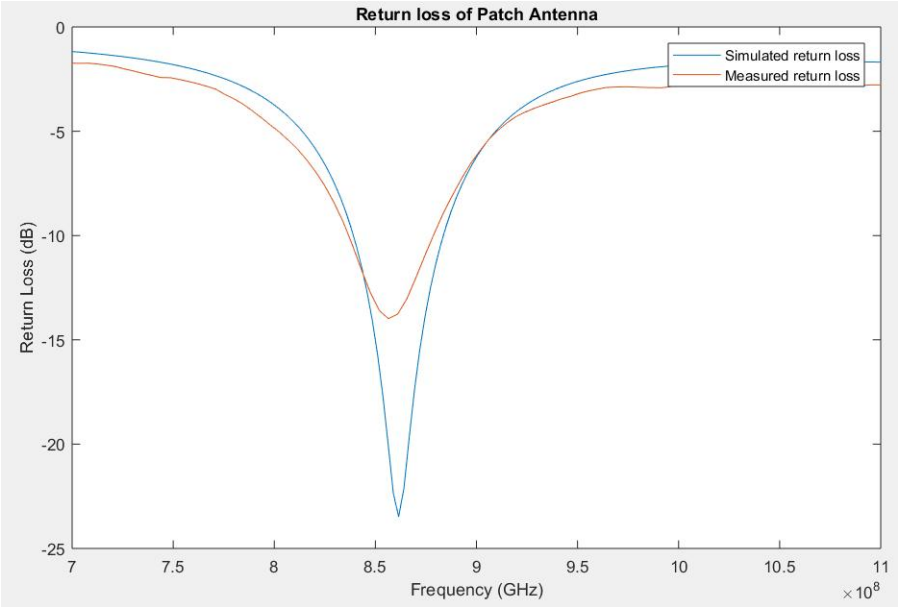

Figure 7-7 *Measured and simulated return loss of slotted patch antenna*

The bandwidth of the measure slotted patch antenna is 20MHz (830-850MHz), which is decreased as compared to its bandwidth in the air 33MHz.

Bending of Slotted Patch Antenna:

The figure 7-8 shows the bending of the slotted patch antenna on the hand.

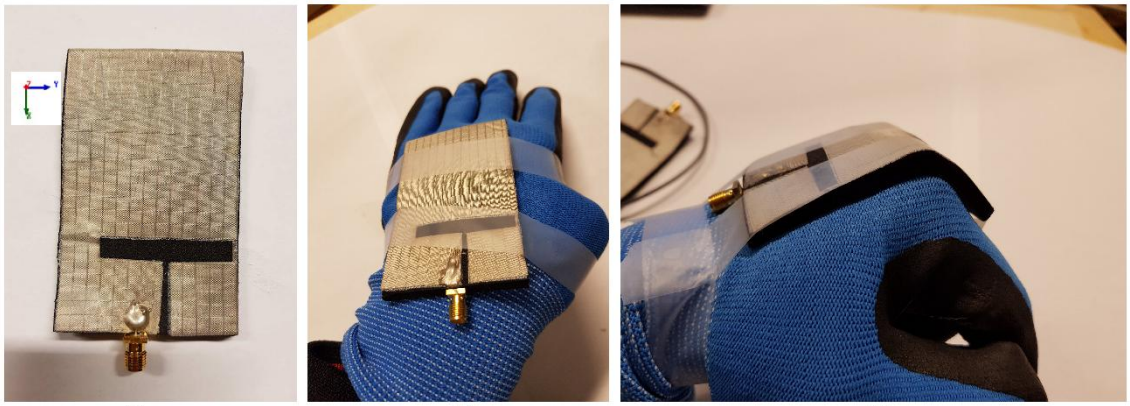

Figure 7-8*(a) Slotted patch antenna in xy-plane (b) bending in yz-plane (c) bending in xz plane*

In the figure 7-8(c) shows the bending of the slotted patch antenna in xz-plane. This can be seen that the impact of the bending on the return loss is not significant but it narrow downs the bandwidth of the antenna. In case of 12mm bending, width and the length of the slot1 and slot2 are changed in the figure 5-10, which results in the significant shift in the resonance frequency.

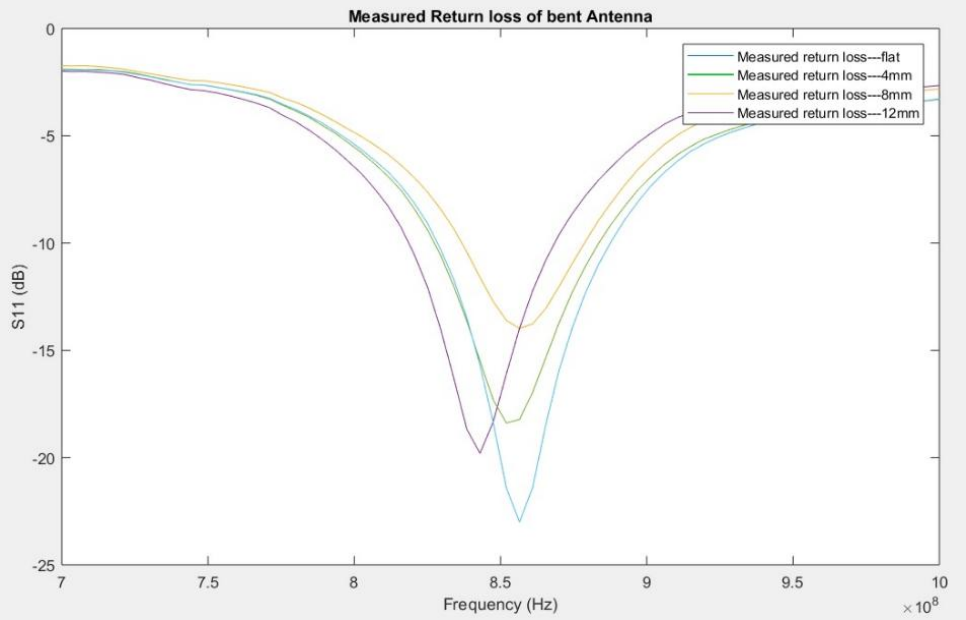

Figure 7-9 *Variation in return loss with antenna bending in xz-plane*

In the figure 7-10 shows the bending of the slotted patch antenna in yz-plane. It can be seen that the bending shifts the resonance frequency to lower bandwidth.

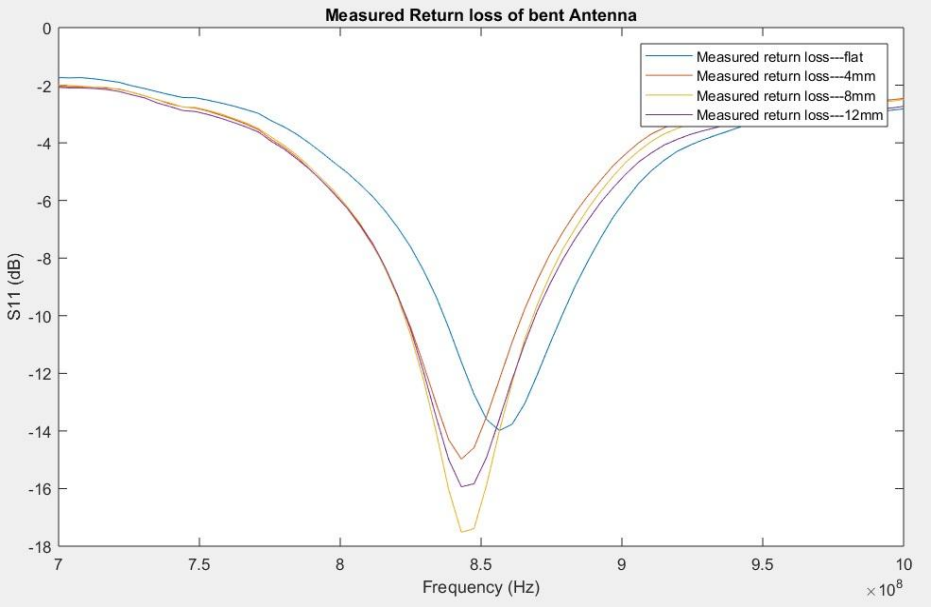

Figure 7-10 *Variation in return loss with antenna bending in yz-plane*

8. COMPARATIVE ANALYSIS

This chapter provides the comparison between different parameters of the SRR and slotted patch antenna. The parameters include the size of the antennas, bending capability, efficiency and the read range of the antennas.

8.1 Size of the Wearable Antennas

When it comes to the size of the SRR and slotted patch antennas, the table 5-2 and 5-2 indicates the maximum size dimensions of the antennas. It can be seen that the SRR antenna is larger in dimensions but the total surface area of the SRR antenna is comparatively less than that of the slotted patch antenna, which makes SRR antenna more wearable than slotted patch antenna. The figure 8-1 shows the size comparison both the antennas. In addition to that, the SRR antenna has a long feeding line which makes more flexible and less chances for the RF connector to get damaged.

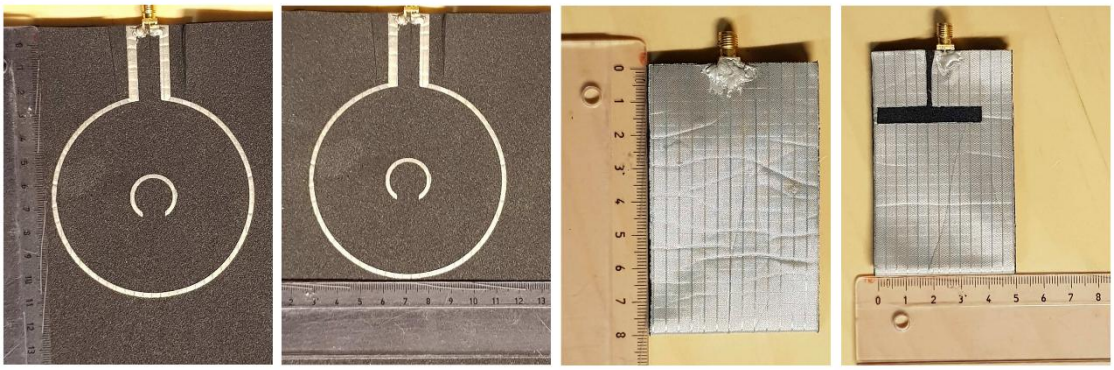

Figure 8-1 *(a) Length of the SRR antenna (b) Width of the SRR antenna (c) Length of the slotted patch antenna (d) Width of the slotted patch antenna*

8.2 Bending Capability

For the wearable antennas, the bending capability is of key importance to avoid any hindrance in the movement of the hand. Therefore, antenna should be more flexible and should have good bending capability. As the SRR antenna is fabricated on a 3mm EPDM foam substrate, whereas, the slotted patch antenna is fabricated on a 4mm EPDM foam substrate. Furthermore, the SRR antenna has less surface area of the conductive textile than the slotted patch antenna. Due to these reason, the bending of the SRR antenna is more practical as compared to the slotted patch antenna. The figure 8-2 shows the bending of the both the antennas and it can be seen that the SRR antenna bends smoothly whereas the slotted patch antenna is not capable of bending itself in proper geometry.

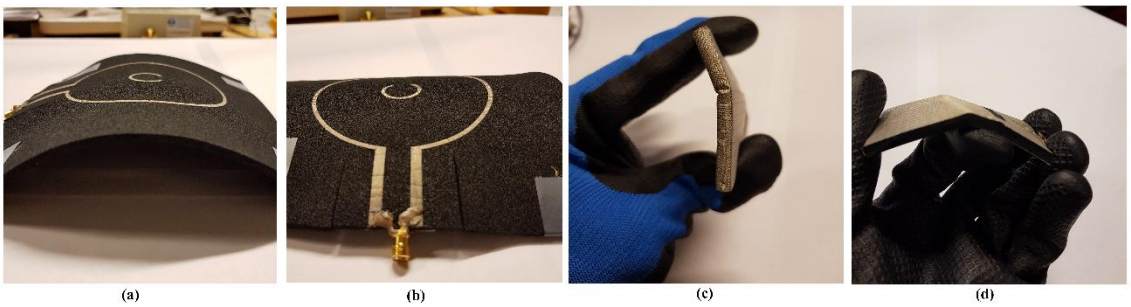

Figure 8-2 *Comparison of bending of both antennas (a)(b) Bending of the SRR antenna (c)(d) Bending of the slotted patch antenna*

8.3 Radiation Efficiency

The efficiency is an important parameter of the wearable antenna as it can affect the performance of the antennas. Figure 8-3 represents the simulated radiation efficiency comparison of both the antennas on human hand. It can be seen that the SRR antenna has more radiation efficiency at 860MHz as compared to the slotted patch antenna. The reason is because the SRR antenna has less radiating surface area, hence, the interaction between the radiating element of the antenna and body is comparatively less. This makes the human body to have less influence on the current path within the radiating element of the antenna.

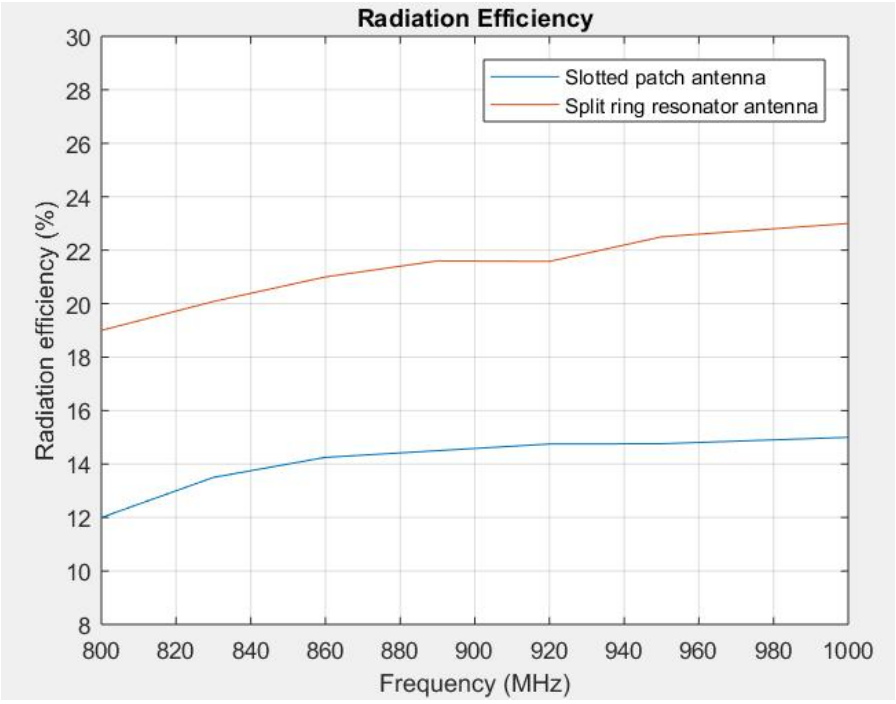

Figure 8-3 *Simulated radiation efficiency comparison of slotted patch antenna and SRR antenna in free space*

8.4 Read Range

As both the antennas are designed as RFID reader antenna, therefore, it is important to compare the read ranges of the antennas. Figure 8-4 shows the comparison of the read ranges of both the antennas. Antennas are attached to the voyantic tagformance equipment to measure test response of the antennas and "Wideband UHF Reference Tag V1"—shown in the figure 8-4—is read with both the antennas. It is evident from the figure 8-4, slotted patch antenna has shown slightly more read range than that of the SRR antenna. The slotted patch antenna received -30dB power from a distance of 70cm, whereas, the SRR antenna received the same power from the tag at 50cm distance. The possible reason for this is the slotted patch antenna has a ground plane, which provides good insulation between the antenna and the human body.

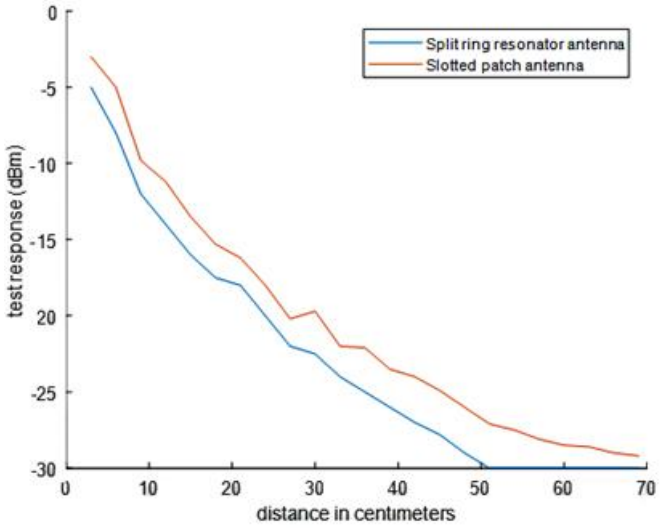

Figure 8-4 *Read range of SRR and slotted patch antenna using the Voyantic Tagformance equipment*

Figure 8-5 *Voyantic Ltd. Wideband UHF Reference Tag v1*

9. CONCLUSION

This chapter concludes the thesis, summarizes the main results and emphasize on the future work than can be done to improve the performance of the antennas.

9.1 Conclusion

In this Master's thesis, the performance evaluation of the wearable antennas by fabricating different type of antennas on the substrate has been discussed. For this purpose, two types of antenna—Split Ring Resonator (SRR) and Slotted Patch Antenna—are selected and fabricated on the EPDM material of thickness 3mm and 4mm respectively. In order to evaluate the performance, both on-body and free space measurements are performed and analyzed. Finally, a detailed comparison of the results are discussed to validate the functionality of the antennas in real environment.

Both the antennas showed good agreement between the simulated and measured free space measurements, however, due to fabrication inaccuracies, the shift in the resonance frequencies of the antennas are observed. In free space measurement, the antennas are bent in xz and yz planes, in order to study the bending effect on the return loss and bandwidth of the antennas. The results concluded that the bending effects the performance of the antennas along the direction, which defines the resonance length of the antennas. The return loss is improved with frequency shifting when the antennas are bent in yz plane.

The near body performance of the designed antennas by mounting the antennas directly on the hand. It is observed that the read range of the antennas is decreased due the influence of the human body. The bending analysis on human body showed improved return loss of the antennas and the bandwidth of the antennas is also improved with bending.

The summary of the results showed that both SRR and slotted patch antennas are operatable for the desired application in order to read the tag in close premises. Although the slotted patch antenna has a slightly greater read range for the reference tag, however, the flexibility of the SRR makes it more convenient to be used for hand glove RFID applications.

10. REFERENCES

[1] M. Kaur, M. Sandhu, N. Mohan and P. S. Sandhu, "RFID technology pinciples, advantages, limitations & its application," International Journal of Computer and Electrical Engineering, 2011.

[2] C. Jechlitschek, "A survey paper on radio frequency identification (rfid) trends," 2013.

[3] Global Language of Business, "Regulatory status for using RFID in the EPC Gen2 (860 to 960 MHz)," 2016.

[4] K. Y. Yazdandoost and R. Miura "Antenna polarization mismatch in ban communications," IEEE, 2013.

[5] A. S. Alqadami, M. F. Jamlos, "Design and development of a flexible and elastic," IEEE APACE, 2014.

[6] E. F. Sundarsingh, S. Velan, M. Kanagasabai al, "Polygon-shaped slotted dual-band antenna for wearable applications," IEEE, 2014.

[7] D. M. Pozar, "Microwave Engineering," John Wiley & Sons Inc, 2005.

[8] M. Sadiku, "The second industrial revolution," 1982.

[9] C. A. Balanis, ""Antenna Theory, Analysis and Design,"3rd ed.," John Wiley & Sons Inc., USA, 1992.

[10] C. A. Balanis, ""Antenna Theory, Analysis and Design," 3rd ed.," John Wiley & Sons Inc., USA, 2005.

[11] J. D. Kraus, R. J. Marhefka, ""Antennas for all applications", 3rd Ed.," USA.

[12] G. A. Thiele, W. L. Stutzman, ""Antenna Theory and Design," 2nd ed.," John Wiley & Sons, USA, 1998.

[13] G. A. Thiele, W. L. Stutzman, "Antenna Theory and Design," John Wiley & sons Inc, USA, 2005.

[14] D. Pozar, "Microwave Engineering," Addison weisley publishing company, USA, 1990.

[15] D. M. Dobkin, "The RF in RFID – Passive UHF RFID in practise.," Elsevier Inc., USA , 2008.

[16] J. Hong, "Wearable computing," HP Labs, Carnegie Mellon Univeristy, 2002.

[17] "G. Marrocco, "The art of UHF RFID antenna design: impedance-matching and size-reduction techniques," in IEEE Antennas and Propagation Magazine, vol. 50, no. 1, pp. 66-79, Feb. 2008.".

[18] "K. Kurokawa, "Power waves and the scattering matrix," in IEEE Transactions on Microwave Theory and Techniques, vol. 13, no. 2, pp. 194-202, Mar 1965.".

[19] H. Stockman, "Communication by Means of Reflected Power," Proc.IRE, 1948.

[20] J. Landt, "The history of RFID," IEEE Potentials, 2005.

[21] "Regulatory status for using RFID in the EPC Gen2 (860-960MHz) band of the UHF spectrum," The global langugage of business, , 30 November 2016, available at: https://www.gs1.org/epcrfid/epc-rfid-uhf-air-interface-protocol/2-0-1

[22] Poole, "RFID frequencies and frequency bands," Available at : http://www.radio-electronics.com/info/wireless/radio-frequency-identification-rfid/low-high-frequency-bands-frequencies.php, Dated : 8.11.2017.

[23] K. V. Seshagiri Rao, "Antenna design for UHF RFID tags: a review and a practical application," IEEE transactions on antennas and propag. , 2005.

[24] Shubin Ma, L. Ukkonen, T. Björninen, “Wearable e-textile split ring passive UHF RFID tag: body-worn performance evaluation,” in Proc. IEEE Asia-Pacific Microwave Conference, 13–16 Nov. 2017, Kuala Lumpur, Malaysia, pp. 166–168

[25] T. Kellomäki, T. Björninen, L. Ukkonen, L. Sydänheimo, "Shirt collar tag for wearable UHF RFID systems," Tampere, 2010.

[26] S. Merilampi, P. Ruuskanen, T. Björninen, L. Ukkonen, L. Sydänheimo, "Printed passive UHF RFID tags as wearable strain sensors," Tampere, 2010.

[27] Y. Hao1, A. Alomainy, P. S. Hall, Y. I. Nechayev, C. G. Parini1, C. C. Constantinou, "Antennas and propagation for body centric wireless communication", 2006.

[28] R. Cavallari, F. Martelli, R. Rosini, "A survey on wireless body area networks," 2011.

[29] P. Salonen, L. Sydänheimo, M. Keskilammi, M. Kivikoski, "A small planar inverted F antenna for wearable application," 1999.

[30] P. Salonen, L.Sydenheimo, "Development of a S-band flexible antenna for smart clothing," 2002.

[31] P. Salonen, L. Hurme, "A novel fabric WLAN antenna for wearable applications," June 2003.

[32] M. Tanaka, J. Jang, "Wearable microstrip antenna," June 2003.

[33] P. Salonen, Y. Rahmat-Samii, M. Kivikoski, "Wearable antennas in the vicinity of the human body," June 2004.

[34] J. B. Pendry, A. J. Holden, D. J. Robbins, and W. J. Stewart, "Magnetism for conductors and enhanced non-linear phenomena," IEEE Trans. Microwave theory technology, 1999.

[35] C. L. Holloway, E. F. Kuester, J. A. Gordon, J. O'Hara, J. Booth, and D. R. Smith, "An overview of the theory and applications of metasurfaces: The two-dimensional Equivalent of metamaterials," IEEE Antennas Propag. Mag., 2012.

[36] P.J. Castro, J. J. Barroso, J. P. L. Neto, "Experimental study on split-ring resonators with different slit widths," Journal of Electromagnetic Analysis and Applications, 2013.

[37] J. Zhou, T. Koschny, and C. M. Soukoulis, "Magnetic and electric excitation in split ring resonators," 2008.

[38] A. Marwaha, R. Rajni, "Role of geometry of split ring resonators in magnetic resonance of metamaterials," International Journal of Electronics and Communication Engineering & Technology (IJECET), 2013.

[39] R. Marqués, F. Mesa, J. Martel, and F. Medina, "Comparative analysis of edge and broadside coupled split ring resonators for metamaterial design-theory and experiments," IEEE Trans, Ant. Propagation, 2003.

[40] A. Tamandani, J. Ahmadi-Shokouh, and S. Tavakoli,, " Wideband planar split ring resonator based metamaterials," Iran, 2013.

[41] R. Marque´s, F. Medina,and R. Rafii-El-Idrissi, "Role of bianisotropy in negative permeability and left-handed metamaterials," Spain, 2002.

[42] M. Klemm, I. Locher, G. Troster, "A novel circularly polarized textile antenna for wearable applications," Electronics Laboratory ETH Zurich, Zurich, Switzerland, 2004.

[43] V. Palanisamy, P. M. Kannan, "Dual band rectangular patch wearable antenna on jean material," International Journal of Engineering and Technology Vol- 3(6), pg 442-446, 2012.

[44] Z. Wei, A. Liu, X. Chen, B. Waris, L. Ukkonen, T. Björninen, and J. Virkki, "Comparison of wearbale passive uhf rfid tags based on electro-textile dipole and patch antennas in body worn comfigurations," Department of Electronics and communication engineering, Tampere University of Technology, Hong kong, 2017.

[45] ANSYS HFSS, "Capabilities," ANSYS HFSS, [Online]. Available: http://www.ansys.com/products/electronics/ansys-hfss/hfss-capabilities. [Accessed 15 11 2017].

[46] italian national research council, "IFAC (Italian national research council), Calculation of the dielectric properties of body tissues in the frequency range of 10Hz-100GHz," Florence, 2015. [Online]. Available: http://niremf.ifac.cnr.it/tissprop/htmlclie/htmlclie.php. [Accessed 2017 11 18].

[47] C. Gabriel, "Compilation of dielectric properties of body tissues at rf and microwave frequencies," London, UK, 1996.

[48] A. Samsuri, "An introduction to polymer science and rubber technology," University Publication Centre (UPENA), 2009.

[49] D. M. Pozar, "“Microwave Engineering,” 3rd ed. John Wiley & Sons Inc.," USA, 2005.

[50] M. Sadiku, "Elements of Electromagnetics, 2nd edition,," Oxford University, 1995.

[51] D. Staelin, "Receivers, antennas, and signals," Massachusetts Institute of Technology, USA, Accessed 9 Nov, 2013.

[52] M. butt, "Systemization of RFID tag antenna design based on optimization techniques and impedance matching charts," Ontario, Canada, 2012.